to target the C-termini of *hdcT* and the N-termini of *hdcA* with an amplicon length of 273 bp. The *hdcA-hisRS* bi-cistronic cDNA was detected by primers 5′-TGC TCA CCA TCT TAC ACA TGA A-3′ and 5′-AAG GCC ATA CCT CAT AGA GAG G-3′, which were designed to target the C-termini of *hdcA* and the N-termini of *hisRS* at an amplicon length of 126 bp. Universal primers 338f and 539r were used to amplify 16S rRNA for an endogenous control.

Reverse transcription of RNAs

RT reactions were carried out using the PrimeScript RT reagent kit (Takara Bio) with 200 ng of total RNA according to the manufacturer instructions.

Amplification

Real-time PCR was performed using the ABI 7900HT sequence-detection system (Applied Biosystems) with 25 μl reaction mixtures containing 12·5 μl of SYBR Premix Ex Taq (Takara Bio), 0·5 μl of ROX (6-carboxy-X-rhodamine, Takara Bio) reference dye, 0·4 μmol l^{-1} each primer, and 2 μl of template cDNA (or known concentrations of genomic DNA) solution with the following thermal protocol: 95°C for 15 s; 40 cycles of 95°C for 10 s and 60°C for 45 s; and an extension phase for dissociation analysis according to manufacturer instructions. All runs included standard templates for calculating a standard curve for amplification efficiency, as well as controls with no reverse transcription and no templates. After confirming amplification specificity by dissociation curve analysis, results were subjected to data analysis as described below. All reaction mixtures were electrophoresed on agarose gels followed by visualization by ethidium bromide staining.

Data analyses

The fluorescent signals were normalized against the reference dye (6-carboxy-X-rhodamine; ROX, included in the SYBR Green buffer) and were used to calculate the ΔRn using Rn^+ (normalized signal)–Rn^- (baseline Rn during cycles 3–15). Data were plotted as ΔRn against the PCR cycle number, with the threshold ΔRn set at 10 times the standard deviation of the mean baseline signal calculated for Rn^-. The threshold cycle (Ct) was defined as the cycle number at which ΔRn fluorescence crossed the threshold for a sample. The standard curve between Ct and the amount of DNA for each primer pair was drawn using 10-fold serial dilutions of genomic DNA and used to calculate the amount of mRNA in each sample. To correct for the total cell number in the RNA extraction and extraction efficiency, the quantity of 16S rRNA in each sample was used for the endogenous control, assuming that the expression of 16S rRNA is constant for all cells used in this mRNA expression analysis.

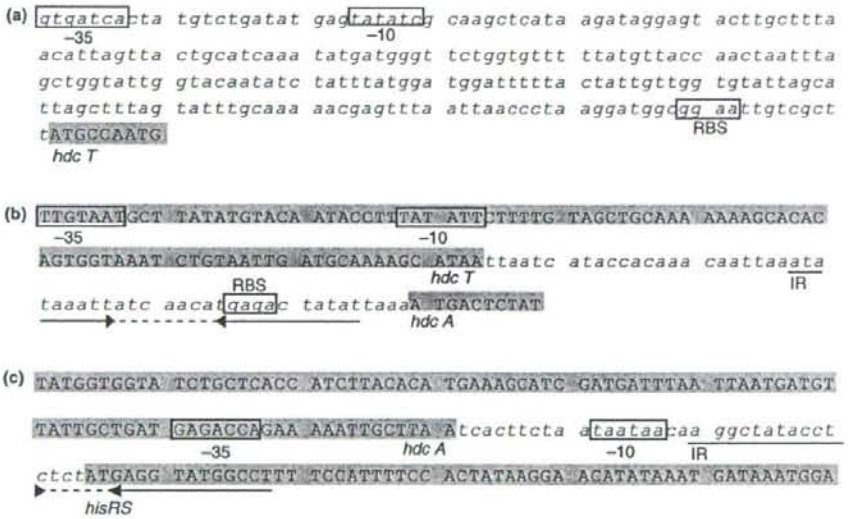

Figure 2 The abstracted representation of the upstream region of the *hdcT* gene (a), *hdcT-hdcA* intergenic region (b), and *hdcA-hisRS* intergenic region (c). Protein coding regions are shown in capital letters on grey background. Putative promoter elements and putative ribosomal binding sites (RBS) are indicated by boxes. The putative transcriptional terminator elements (inverted repeat, IR) are indicated by solid arrows (stems) and dashed lines (loops).

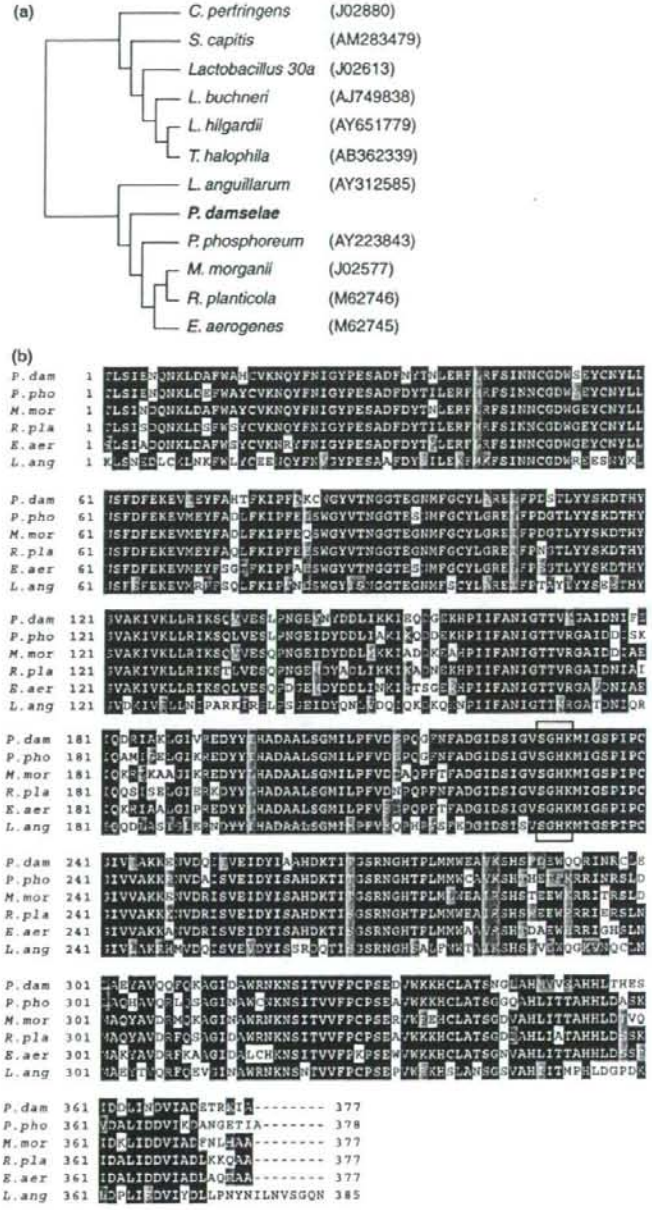

Figure 3 (a) Phylogenetic relationships of bacteria based on deduced HdcA amino acid sequences. Distances between sequences were calculated by ClustalW software (excluding the alignment gaps) and dendrograms were drawn by the neighbour-joining method. The nucleotide sequence accession numbers are shown in parenthesis. (b) Amino acid sequence alignment of HdcA in the following bacteria: P. dam, *Photobacterium damselae*; P. pho, *P. phosphoreum*; M. mor, *Morganella morganii*; R. pla, *Raoultella planticola*; E. aer, *Enterobacter aerogenes*; and L. ang, *L. anguillarum*. Identical residues (white letters on black background) and similar residues (white letters on grey background) are indicated.

Nucleotide sequence accession number

The 6083-bp nucleotide sequence of *P. damselae hdc* gene cluster determined in this study has been submitted to the DDBJ database under accession no. AB363972.

Results

Isolation and sequencing of the *hdc* and related genes of *P. damselae*

Amino acid sequencing of the subunits of the purified histidine decarboxylase of *P. damselae* (TLSIENQNKLDAFWAHCVKNQYFNI) revealed the N-terminal sequence to be highly similar to previously reported histidine decarboxylase sequences of *M. morganii, R. planticola* and *E. aerogenes* (Vaaler *et al.* 1986; Kamath *et al.* 1991). Cloning the 4·5kb *Sac*I–*Sal*I fragment after Southern blot hybridization analysis first revealed *hdcT*, *hdcA* and incomplete ORFs (Fig. 1); therefore, two adjacent fragments were cloned. In total, we sequenced 6083 bp around the *hdcA* gene and found three open reading frame (ORF) sequences and one 3′ partial ORF (>1311 bp) on the same strand. We designated these three ORFs as *hdcT*, *hdcA* and *hisRS*, respectively (Fig. 1). A 3′ partial ORF found at 808-bp upstream of *hdcT* was designated as *orf4*.

Sequence analysis of the *hdc* cluster from *P. damselae*

hdcA

The putative histidine decarboxylase gene, designated as *hdcA* in *P. damselae*, is 1131 bp in length with an initial start codon (ATG) and a stop codon (TAA) at the 3′-end followed by a 12-base inverted repeat, which represents a potential transcription termination site (Fig. 2c). A putative ribosome binding site sequence (dGAGA) is located 10-bp upstream of the translational start codon for *hdcA* (Fig. 2b). The G + C content of the gene was 44% and the molecular weight of the encoded polypeptide of 42 833 Da compares well with earlier reports for subunits of this enzyme from other known *Enterobacteriaceae* (Kamath *et al.* 1991).

The deduced amino acid sequence of *P. damselae* HdcA shares significant sequence similarity with those of *P. phosphoreum, M. morganii, R. planticola, E. aerogenes* and *L. anguillarum* (Fig. 3b). Each enzyme contains 377 or 378 amino acid residues with an overall high sequence similarity of 80%; the lowest similarity is observed in regions between residues 141 and 193 and residues 279–319 (Fig. 3b). Comparison with known decarboxylases revealed that the important catalytic residue lysine at position 234 (K234), with which that pyridoxal 5′-phosphate forms an internal aldimine (Schiff base linkage), was found in HdcA of *P. damselae*. The residues around K234, Ser-Gly-His were conserved in PLP-dependent histidine decarboxylases (Vaaler *et al.* 1986; Kamath *et al.* 1991) (Fig. 3b).

hdcT

This 1143-bp ORF positioned at 43-bp upstream of *hdcA* initiation codon shows the most significant similarity to HdcT compared to membrane proteins, putative amino acid permease of *Salmonella* Paratyphi A and putrescine/ornithine antiporter of *Salmonella* chorelaesuis based on BLAST program search (58% similarity and 38% identity, based on deduced amino acid sequence).

To understand the physiological role of *hdcT*, the hydrophobicity profile of HdcT and other well characterized amino acid/amine antiporters (HdcC of *Lactobacillus buchneri*, HdcP of *Staphylococcus capitis*, and PotE and CadB of *E. coli*) were determined (Fig. 4a). Although the numbers of hydrophobic domains differed between these five proteins, HdcT showed hydrophobic patterns similar to those of the other membrane proteins. The total number of transmembrane spans in the predicted structure of *P. damselae* HdcT is 10 or 11, depending on whether the Serine residue at position 345 was regarded as a transmembrane domain or not, and similar transmembrane regions were observed at the second to sixth transmembrane domains based on comparisons with other amino acid/amine antiporter proteins (Fig. 4b).

hisRS

The deduced amino acid sequence of *hisRS*, located 33 bp downstream of the stop codon of *hdcA* gene, showed significant similarity to histidyl-tRNA synthetase of several bacteria, such as *Haemophilus* sp., *Yersinia* sp. and *Vibrio* sp., ranging from 71% to 68% (data not shown).

Amino acid sequence comparison between HisRS of *P. damselae* and histidyl-tRNA synthetase of *E. coli* (Arnez *et al.* 1995; Guth and Francklyn 2007) identified three conserved motifs of class II aminoacyl-tRNA synthetase (Fig. 5, motifs 1–3). The residues R127, Q129 and R132 were reported to enforce the specificity of histidyl-tRNA synthetase for histidyl-tRNA of *E. coli* (Guth and Francklyn 2007). The conserved residues at positions 268–276, indicated by solid stars in Fig. 5, comprising one wall of the histidine binding pocket in *E. coli* (Arnez *et al.* 1995). According to Arnez *et al.* (1995), the conserved domain at positions 296–303 comprises the floor and back pocket of histidine substrate.

orf4

The closest matches produced by the BLAST search for the deduced amino acid sequence of the 3′ partial ORF

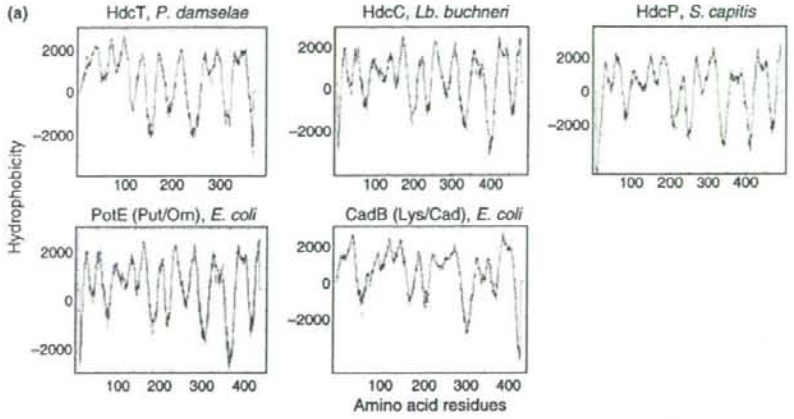

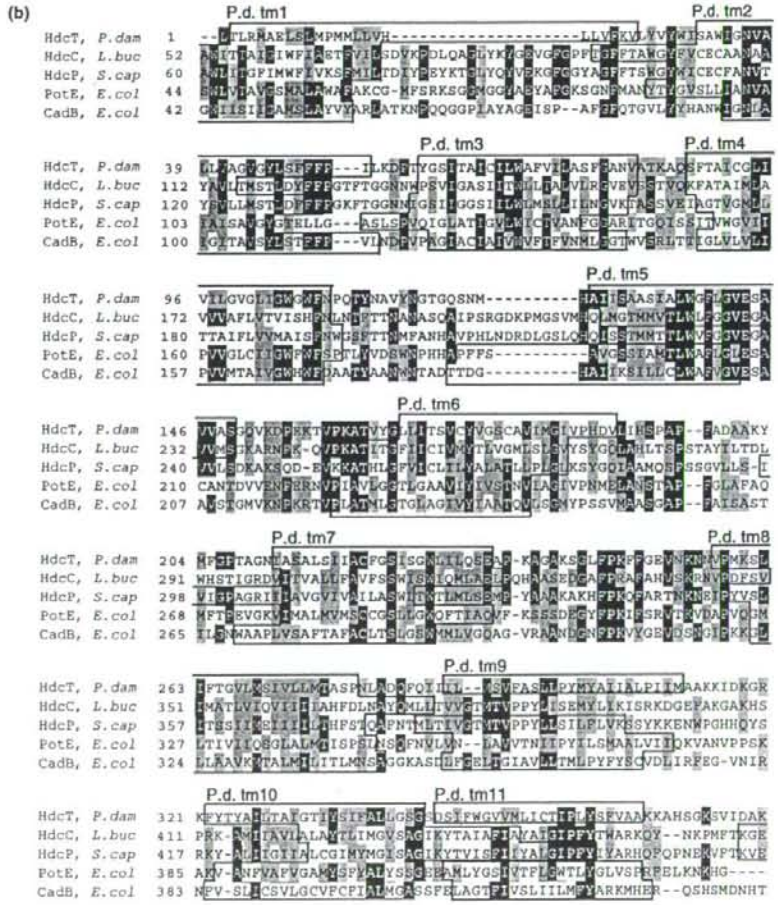

Figure 5 Alignment of the deduced amino acid sequence for *hisRS* of *Photobacterium damselae* and histydyl-tRNA synthetase of *Escherichia coli*. The identical (white letters on black background) and similar (white letters on grey background) amino acid residues are indicated. The significantly conserved domains of class II aminoacyl-tRNA synthetase protein are boxed (motifs 1–3). Open stars indicate important residues for specificity of histidyl-tRNA synthetase to histidyl-tRNA molecules in *E. coli* (Guth and Francklyn 2007). Closed stars and grey bar indicate domains related to the interaction of histidine substrate with histidyl-tRNA synthetase in *E. coli* (Arnez *et al.* 1995).

(>1311 bp) found 808 bp upstream of the *hdcT* start codon were putative helicases from various sources, such as *Shewanella oneidensis* (76% similarity, AE014299) and *Vibrio chorelae* (75% similarity, EDL74353).

Expression of *hdc* gene in *E. coli*

To confirm the function of the *hdcA* gene, histamine excretion was measured in cultures of *E. coli* cells harbouring plasmids pSS45 (containing *hdcT* and *hdcA*), pSK18 and pSK19. Plasmids pSK19 and pSK18 contained only the complete *hdcA* ORF under control of the *lac* promoter and in the opposite orientation to the *lac* promoter, respectively (Table 1). After 5 h of incubation, the transformants harbouring pSK18 and pSK19 produced histamine at 18·4 ppm and 26·6 ppm, respectively. The transformant harbouring pSS45 produced histamine at a concentration of 916 ppm (Fig. 6). In cultures of *E. coli* BL21 (DE3) harbouring the pUC 18 vector alone, no histamine was detected.

Transcriptional analysis of *hdc* operon

Northern blot with labelled *hdcA* gene fragments showed a major *hdcA*-hybridizing band corresponding to the 1·25-kb transcript, at both pH 4·5 and 7·5 (Fig. 7a). The size corresponds to the predicted size for the *hdcA* monocistronic transcript. Another hybridizing band, with a size of 2·5 kb, was detected from cells cultured with histidine at pH 4·5 or pH 7·5 (Fig. 7a). The fragment sizes corresponded to those predicted for *hdcT-hdcA* or *hdcA-hisRS* co-transcripts. Similar expression patterns were observed for the use of partial DNA of *hdcT* as a probe; a 1·25 kb band for *hdcT* monocistronic transcript and the 2·5 kb

Figure 4 Comparison of the HdcT and other amino acid/amine antiporters. (a) Hydrophobicity plots calculated using TMpred. (b) Multiple sequence alignment of the deduced amino acid sequences. Amino acid residues identical (white letters on black background) and similar (white letters on grey background) for more than three sequences per site are indicated. Predicted transmembrane domains of HdcT of *Photobacterium damselae*, HdcC of *Lactobacillus buchneri* (AJ749838) and HdcP of *S. capitis* (AM283479) using SOSUI program, and that of previously reported PotE (putrescine/ornithine antiporter, Kashiwagi *et al.* 1999) and CadB (lysine/cadaverine antiporter, Soksawamakhin *et al.* 2005) of *Escherichia coli* are indicated by boxes.

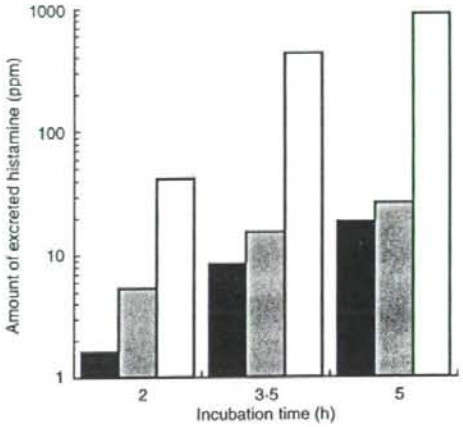

Figure 6 Expression of *hdcA* or *hdcT-hdcA* genes of *Photobacterium damselae* in *Escherichia coli* BL21 (DE3). Fragments containing only *hdcA* or both *hdcA* and *hdcB* were subcloned into pUC18/19 plasmid vectors followed by transformation into *E. coli* BL21 (DE3) to obtain pSK18-DE3 (solid bars, containing *hdcA* gene in the opposite orientation to the *lac* promoter), pSK19-DE3 (grey bars, containing *hdcA* gene under control of the *lac* promoter) and pSS45-DE3 (open bars, containing both *hdcA* and *hdcB* genes under control of the *lac* promoter). Transformants were cultured in LB medium containing 1% l-histidine and 1 mmol l^{-1} IPTG, and culture supernatants were then collected and the concentration of histamine was measured. In cultures of *E. coli* BL21 (DE3) harbouring only the pUC 18 vector, no histamine was detected.

band correspond to *hdcT-hdcA* transcript were detected as a major band at pH 4·5 (Fig. 7a). Under the incubation condition of pH 4·5 with histidine, the 4·0 kb transcript, corresponded to the *hdcT-hdcA-hisRS* tri-cistronic transcript was observed with both of *hdcT* and *hdcA* probes (Fig. 7a). To summarize, six types of transcripts were detected from *P. damselae hdc* gene cluster: *hdcT*, *hdcA*, *hisRS*, *hdcT-hdcA*, *hdcA-hisRS* and *hdcT-hdcA-hisRS*. Transcript number was higher at pH 4·5 than pH 7·5, and under histidine excess (Fig. 7a).

To precisely compare the expression ratio among these conditions, quantitative RT-PCR was performed. The most abundant transcripts of each genes were detected at pH 4·5 with histidine excess (Fig. 7b, hatched bars). The expression of each gene was reduced 10^{-1} to 50^{-1} fold both at pH 4·5 without histidine and at pH 7·5 with histidine excess (Fig. 7b). However, the transcript amount under these conditions was not significantly different, except for *hdcA*, which was slightly higher than the other four ($P < 0{\cdot}05$). On the other hand, at pH 7·5 without addition of histidine, all of these genes showed significantly less transcription than under the other conditions. At pH 7·5 without addition of histidine, *hisRS* mRNA was most abundant with *hdcT* and *hdcA* at 0·73 and 0·38 log difference, respectively.

Discussion

We isolated and sequenced the histidine decarboxylase gene (*hdcA*), which showed high identity with the amino acid sequences of histidine decarboxylases of other known Gram-negative bacteria: *M. morganii* (79·6% identity), *R. planticola* (79·1%), and *E. aerogenes* (76·9%) (Vaaler *et al.* 1986; Kamath *et al.* 1991); *P. phosphoreum* (80·2%, Morii *et al.* 2006); and *P. damselae* (100%, Kanki *et al.* 2007) (Fig. 3). The deduced amino acid sequence of HdcA was comprised of the determined N-terminal amino acid sequence with the exception of a methionine at the first residue. The first methionine was presumed to be removed at maturation, as has previously been shown for other HdcA of *R. planticola* and *E. aerogenes* (Guirard and Snell 1987; Kamath *et al.* 1991). These pyridoxalphosphate dependent histidine decarboxylase genes, which are distributed among Gram-negative bacteria, are thought to have evolved from a common ancestral gene (Fig. 3a).

To confirm the function of the *hdcT* and *hdcA* genes of *P. damselae*, *hdcA or hdcT-hdcA* genes were expressed in *E. coli*. Plasmids containing the *hdcA* gene enabled the transformed *E. coli* strain to produce histamine (Fig. 6); therefore, we concluded that *hdcA* encodes histidine decarboxylase. Histamine concentration in cultures of recombinants harbouring pSS45 was almost 50 times greater than in cultures of recombinants harbouring pSK19 in IPTG-induced conditions, indicating that *hdcT*, an upstream genetic element of *hdcA* has a positive effect for either *hdcA* expression level or the excretion level of histamine. The hydrophobicity of the amino acid sequence of HdcT (Fig. 3a) suggests that HdcB is located in the cytoplasmic membrane. The sequence alignment and comparison of predicted transmembrane domains between well characterized amino acid/amine antiporters, PotE (Kashiwagi *et al.* 2000) and CadB (Soksawatmaekhin *et al.* 2006) (Fig. 3b) support this finding. Moreover, comparison of HdcT between other amino acid/amine antiporters revealed several conserved residues of histidine/histamine antiporter proteins from Gram-positive bacteria. Therefore, HdcT is strongly suggested to be a histidine/histamine antiporter in *P. damselae*. This is consisted with the observation of larger amounts of histamine in cultures of *E. coli* harbouring pSS45 (containing both of *hdcT* and *hdcA*) than in cultures of *E. coli* harbouring pSK18/19 (containing *hdcA*).

Northern blot experiments and quantitative RT-PCR revealed the *hdc* genes were highly induced under acidic

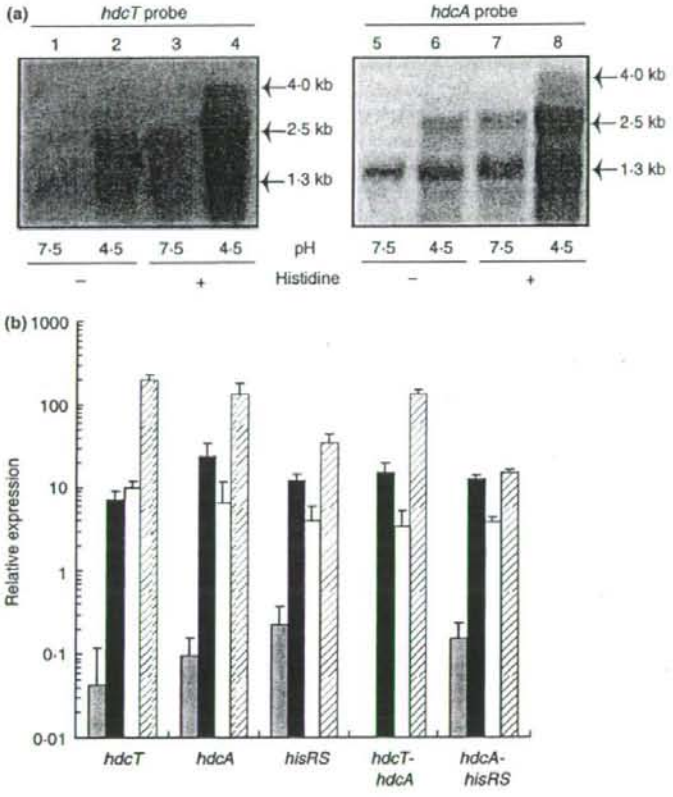

Figure 7 Transcriptional analyses of the *hdc* genes of *P. damselae* under different culture conditions. (a) Northern blot hybridization. Lanes 1 and 5, pH 7·5; lane 2 and 6, pH 4·5; lane 3 and 7, pH 7·5 with histidine; lane 4 and 8, pH 4·5 with histidine. Aliquots (20 μg) of total RNA were electrophoresed and blotted to membranes followed by hybridization with *hdcT* (lanes 1–4) or *hdcA* (lanes 5–8) probes. (b) Quantification of mRNA extracted from cells treated with pH 7·5 (grey bars), pH 4·5 (solid bars), pH 7·5 with histidine (white bars), and pH 4·5 with histidine (hatched bars). cDNA was quantified against a standard curve produced using genomic DNA. The relative amount of 1 is approx. equal to 10^3 copies of genomic DNA per reaction. Bars represent the averages of three experiments, and error bars indicate the SD.

conditions or histidine-rich condition, or both. Both mono- and poly-cistronic transcription were observed. The intense band corresponding to a 2·5-kb transcript at pH 4·5 in the presence of histidine, as revealed by both *hdcA* and *hdcT* probes, indicates that the *hdcTA* co-transcript is a major transcriptional product under this condition and these were also evidenced by RT-PCR. On the other hand, *hdcTA* transcription was not detected under pH 7·5 without histidine condition (Fig. 7b), while both mono-cistronic *hdcT* and *hdcA* mRNA were detected. This is consistent with previous reports of *cadBA* operon of *V. cholerae* (Merrell and Camilli 2000). However, the reason for transcription of these *hdc* genes as either bi- or mono-cistronic messages remains to be elucidated. Morii and Kasama (1995, 2004) and Morii *et al.* (2006) reported that the decarboxylation of histidine by *P. phosphoreum* was achieved by two types of histidine decarboxylase enzymes (constitutive and inducible), which could be separated and fractionated by gel chromatography. However, our Southern hybridization results using different enzyme combinations showed that a single *hdc* gene was present on the chromosome of *P. damselae* (data not shown). The presence of *hdcT* and *hdcA* monocistronic transcripts at an amount almost 100-fold greater than under acidic or histidine excess condition (Fig. 7b) indicates that the *hdcA* gene was expressed constitutively in *P. damselae* although at lower amounts than under low pH or histidine excess conditions.

It is interesting that the *hisRS* gene, the putative histidyl-tRNA synthetase gene, was found immediately downstream

(33 bp) of the 3′ end of *hdcA*. This organization was comparable with the well characterized *hdc* gene cluster of *Lb. buchneri* (Martine *et al.* 2005). In *P. damselae*, *hisRS* was induced at pH 4·5 and histidine excess (Fig. 7b); however, the reason for induction of *hisRS* expression under higher concentration of extracellular histidine remains unknown. One possible explanation is co-transcription of *hdcA* to *hisRS*, which is caused by the incomplete action of the transcriptional terminator of upstream genes, similar to that of the *tdc* operon of *E. faecalis* (Connil *et al.* 2002).

The *cad* operon, which encodes the lysine decarboxylation pathway, has been proposed to function in the pH homeostasis system of *Salmonella* (Foster and Hall 1990) and some of *Vibrio species* (Merrell and Camilli 2000; Rhee *et al.* 2002; Tanaka *et al.* 2008). According to the model proposed in those reports, lysine is taken up vigorously and is quickly turned over to cadaverine and CO_2, which can freely escape through the cell membrane to the atmosphere. Thus, the reaction could eliminate a large quantity of H^+ ions from the cell. It is reasonable to assume that histidine and histamine in *P. damselae* might play a role in acid survival similar to the roles of lysine and cadaverine because the transcription of *hdcT* and *hdcA* genes were significantly enhanced under acidic (pH 4·5) condition similar to elevated *cad* operon transcription under acidic condition (Merrell and Camilli 2000; Rhee *et al.* 2002; Tanaka *et al.* 2008).

In conclusion, we clarified the mechanism of histamine formation by *P. damselae*. Two enzymes were shown to be involved in producing histamine: histidine decarboxylase (*hdcA*) and putative histidine/histamine antiporter (*hdcT*), which takes histidine into the cytoplasmic space and excretes histamine from the cell. The transcripts of these genes were increased under conditions of low pH and the presence of extracellular histidine. Accumulation of histamine by *P. damselae* may confer resistance to acid stress developed through consuming intracellular protons via the decarboxylation reaction, as reported in other bacterial species (Park *et al.* 1996; Cornet *et al.* 2001; Merrell and Camilli 2002).

Acknowledgements

This work was partly supported by the Japanese Ministry of Health, Labour and Welfare (H20-011). The authors thank for Masataka Satomi, Kazuo Shiomi and Yuji Nagashima for helpful dilscussions, and also thank for Masami Ishida for conducting protein purification.

References

Altschul, S.F., Madden, T.L., Schaffer, A.A., Zhang, J., Zhang, Z., Miller, W. and Lipman, D.J. (1997) Gapped BLAST and PSI-BLAST: a new generation of protein database search programs. *Nucleic Acids Res* 25, 3389–3402.

Arnez, J.G., Harris, D.C., Mitschler, A., Rees, B., Francklyn, C.S. and Moras, D. (1995) Crystal structure of histidyl-tRNA synthetase from *Escherichia coli* complexed with histidyl-adenylate. *EMBO J* **14**, 4143–4155.

Bearson, S., Bearson, B. and Foster, J.W. (1997) Acid stress responses in enterobacteria. *FEMS Microbiol Lett* **147**, 173–180.

Castanie-Cornet, M.P., Penfound, T.A., Smith, D., Elliott, J.F. and Foster, J.W. (1999) Control of acid resistance in *Escherichia coli*. *J Bacteriol* **181**, 3525–3535.

Connil, N., Breton, Y.L., Dousset, X., Auffray, Y., Rince, A. and Prevost, H. (2002) Identification of the *Enterococcus faecalis* tyrosine decarboxylase operon involved in tyramine production. *Appl Environ Microbiol* **68**, 3537–3544.

Cotter, P.D., Gahan, C.G. and Hill, C. (2001) A glutamate decarboxylase system protects *Listeria monocytogenes* in gastric fluid. *Mol Microbiol* **40**, 465–475.

Foster, J.W. and Hall, H.K. (1990) Adaptive acidification tolerance response of Sal*monella typhimurium*. *J Bacteriol* **172**, 771–778.

Guirard, B.M. and Snell, E.E. (1987) Purification and properties of pyridoxal-5′-phosphate-dependent histidine decarboxylases from *Klebsiella planticola* and *Enterobacter aerogenes*. *J Bacteriol* **169**, 3963–3968.

Guth, E.C. and Francklyn, C.S. (2007) Kinetic discrimination of tRNA identity by the conserved motif 2 loop of a class II aminoacyl-tRNA synthetase. *Mol Cell* **25**, 531–542.

Hirokawa, T., Boon-Chieng, S. and Mitaku, S. (1998) SOSUI: classification and secondary structure prediction system for membrane proteins. *Bioinformatics* **14**, 378–379.

Hofmann, K. and Stoffel, W. (1993) TM base – a database of membrane spanning proteins segments. *Biol Chem Hoppe-Sayler* **374**, 166.

Kamath, A.V., Vaaler, G.L. and Snell, E.E. (1991) Pyridoxal phospate-dependent histidine decarboxylase-cloning, sequencing, and expression of genes from *Klebsiella planticala* and *Enterobacter aerogenes* and properties of the overexpressed enzymes. *J Biol Chem* **266**, 9432–9437.

Kanki, M., Yoda, T., Tsukamoto, T. and Baba, E. (2007) Histidine decarboxlylases and their role in accumulation of histidine in tuna and dried saury. *Appl Environ Microbiol* **73**, 1467–1473.

Kashiwagi, K., Kuraishi, A., Tomitori, H., Igarashi, A., Nishimura, K., Shirahata, A. and Igarashi, K. (2000) Identification of the putrescine recognition site on polyamine transport protein PotE. *J Biol Chem* **275**, 36007–36012.

Kimura, B., Hokimoto, S., Takahashi, H. and Fujii, T. (2000) *Photobacterium histaminum* Okuzumi *et al.* 1994 is a later subjective synonym of *Photobacterium damselae* subsp. *damselae* (Love *et al.* 1981) Smith *et al.* 1991. *Int J Syst Evol Microbiol* **50**, 1339–1342.

Kurihara, K., Wagatsuma, Y., Fujii, T. and Okuzumi, M. (1993) Effect of culture conditions on L-histidine decar-

boxylation activity of halophilic histamine-forming bacteria. *Nippon Suisan Gakkaishi* **59**, 1401–1406.

Lin, J., Smith, M.P., Chapin, K.C., Baik, H.S., Bennett, G.N. and Foster, J.W. (1996) Mechanism of acid resistance in enrohemorrhagic *Escherichia coli*. *Appl Environ Microbiol* **62**, 3094–3100.

Martine, M.C., Fernandez, D.M., Linares, D.M. and Alvarez, M.A. (2005) Sequencing, characterization and transcriptional analysis of the histidine decarboxylase operon of *Lactobacillus buchneri*. *Microbiology* **151**, 1219–1228.

Meng, S.Y. and Bennett, G.N. (1992a) Nucleotide sequence of the *Escherichia coli cad* operon; a system for neutralization of low extracellular pH. *J Bacteriol* **174**, 2659–2669.

Meng, S.Y. and Bennett, G.N. (1992b) Regulation of the *Escherichia coli cad* operon: Location of the site required for acid induction. *J Bacteriol* **174**, 2670–2678.

Merrell, D.S. and Camilli, A. (1999) The *cadA* gene of *Vibrio cholerae* is induced during infection and plays a role in acid tolerance. *Mol Microbiol* **34**, 836–849.

Merrell, D.S. and Camilli, A. (2000) Regulation of *Vibrio cholerae* genes required for acid tolerance by a member of the "ToxR-like" family of transcriptional regulators. *J Bacteriol* **182**, 5342–5350.

Merrell, D.S. and Camilli, A. (2002) Acid tolerance of gastrointestinal pathogens. *Curr Opin Microbiol* **5**, 51–55.

Morii, H. and Kasama, K. (1995) Changes in the activity of two histidine decarboxylases from *Photobacterium phosphoreum* during growth under different oxygen tensions. *Fish Sci* **61**, 845–851.

Morii, H. and Kasama, K. (2004) Activity of two histidine decarboxylases from *Photobacterium phosphoreum* at different temperatures, pHs, and NaCl concentrations. *J Food Prot* **67**, 1736–1742.

Morii, H., Kasama, K. and Herrera-Espinoza, R. (2006) Cloning and sequencing of the histidine decarboxylase gene from *Photobacterium phosphoreum* and its functional expression in *Escherichia coli*. *J Food Prot* **69**, 1768–1776.

Murray, M.G. and Thompson, W.F. (1980) Rapid isolation of high molecular weight plant DNA. *Nucl Acids Res* **8**, 4321–4325.

Okuzumi, M., Okuda, S. and Awano, M. (1981) Isolation of psychrophilic and halophilic histamine-forming bacteria from *Scomber japonicus*. *Bull Jpn Soc Sci Fish* **47**, 1591–1598.

Okuzumi, M., Hiraishi, A., Kobayashi, T. and Fujii, T. (1994) *Photobacterium histaminum* sp. nov., a histamine-producing marine bacterium. *Int J Syst Bacteriol* **44**, 631–636.

Park, T.K., Bearson, B., Bang, S.H., Bang, I.S. and Foster, J.W. (1996) Internal pH crisis, lysine decarboxylase and the acid tolerance response of *Salmonella typhimurium*. *Mol Microbiol* **20**, 605–611.

Rhee, E.R., Rhee, J.H., Ryu, P.Y. and Choi, S.H. (2002) Identification of the *cadBA* operon from *Vibrio vulnificus* and its influence on survival to acid stress. *FEMS Microbiol Lett* **208**, 245–251.

Sambrook, J.E., Fritsch, F. and Maniatis, T.S. (1989) *Molecular Cloning: A Laboratory Manual*, 2nd edn. Cold Spring Harbor, New York: Cold Spring Harbor Laboratory.

Sanders, J.W., Leenhouts, K., Burghoorn, J., Brands, J.R., Venema, G. and Kok, J. (1998) A chloride-inducible acid resistance mechanism in *Lactococcus lactis* and its regulation. *Mol Microbiol* **27**, 299–310.

Soksawatmaekhin, W., Uemura, T., Fukiwake, N., Kashiwagi, K. and Igarashi, K. (2006) Identification of the cadaverine recognition site on the cadaverine-lysine antiporter CadB. *J Biol Chem* **281**, 29213–29220.

Tanaka, Y., Kimura, B., Takahashi, H., Watanabe, T., Obata, H., Kai, A., Morozumi, S. and Fujii, T. (2008) Lysine decarboxylase of *Vibrio parahaemolyticus*: kinetics of transcription and role in acid resistance. *J Appl Microbiol* **104**, 1283–1293.

Thompson, J.D., Higgins, D.G. and Gibson, T.J. (1994) Clustal W: improving the sensitivity of progressive multiple sequence alignment through sequence weighting, positions-specific gap penalties and weight matrix choice. *Nucleic Acids Res* **22**, 4673–4680.

Vaaler, G.L., Brash, M.A. and Snell, E.E. (1986) Pyridoxal 5′-phosphate-dependent histidine decarboxylase-nucleotide sequence of the *hdc* gene and the corresponding amino acid sequence. *J Biol Chem* **261**, 11010–11014.

Waterman, S.R. and Small, P.L.C. (1996) Identification of σ^S-dependent genes associated with the stationary-phase acid-resistance phenotype of *Shigella flexneri*. *Mol Microbiol* **21**, 925–940.

Watson, N., Dunyak, D.S., Rosely, E.L., Slonczewoski, J.L. and Olson, E.R. (1992) Identification of elements involved in transcriptional regulation of the *Escherichia coli cad* operon by external pH. *J Bacteriol* **174**, 530–540.

Yamanaka, H. and Matsumoto, M. (1989) Simultaneous determination of polyamines in red meat fishes by high performance liquid chromatography and evaluation of freshness. *J Food Hyg Soc Jpn* **30**, 396–400.

Yamane, K., Asato, J., Kawade, N., Takahashi, H., Kimura, B. and Arakawa, Y. (2004) Two cases of fatal necrotizing facilities caused by *Photobacterium damselae*. *J Clin Microbiol* **42**, 1370–1372.

Yanisch-Perron, C., Vieira, J. and Messing, J. (1985) Improved M13 phage cloning vectors and host strains: nucleotide sequences of the M13mp18 and pUC19 vectors. *Gene* **33**, 103–119.

Microbial Pathogenesis 45 (2008) 150–158

Contents lists available at ScienceDirect

Microbial Pathogenesis

journal homepage: www.elsevier.com/locate/micpath

Difference of genotypic and phenotypic characteristics and pathogenicity potential of *Photobacterium damselae* subsp. *damselae* between clinical and environmental isolates from Japan

Hajime Takahashi [a], Satoko Miya [a], Bon Kimura [a,*], Kunikazu Yamane [b], Yoshichika Arakawa [b], Tateo Fujii [a,1]

[a] Department of Food Science and Technology, Faculty of Marine Science, Tokyo University of Marine Science and Technology, 4-5-7 Konan, Minato-ku, Tokyo 108-8477, Japan
[b] Department of Bacterial Pathogenesis and Infection Control, National Institute of Infectious Diseases, Tokyo, Japan

ARTICLE INFO

Article history:
Received 8 January 2008
Received in revised form 17 April 2008
Accepted 29 April 2008
Available online 8 May 2008

Keywords:
Photobacterium
Photobacterium damselae subsp. *damselae*
Photobacterium damselae subsp. *piscicida*
Subtyping
Hemolytic activity

ABSTRACT

Photobacterium damselae subsp. *damselae* has been known as an opportunistic pathogen in fish and mammals. Human infectious cases are often very serious and occasionally fatal. We previously reportedtwo fatal cases caused by this subspecies where the patients developed multiple organ failure within 20–36 h after the onset of initial symptoms. Despite its ability to cause serious infections in humans, this subspecies has not been well studied because human infectious cases caused by this subspecies are very rare. However, this subspecies has been reported to be present in a wide range with high incidence rate in aquatic environments. Thus, we investigated the genotypic and phenotypic differences between clinical and environmental strains of *Photobacterium damselae* subsp. *damselae*. Using molecular typing methods, such as ribotyping, AFLP (Amplified Fragment Length Polymorphism), and PFGE (Pulsed-Field Gel Electrophoresis) and sequencing analysis, we determined that thetwo clinical strains were genetically similar yet distinguishable from environmental strains, but not significantly so. On the other hand, phenotypic differences were clear; moreover, mouse assay and hemolytic assay indicated strong pathogenicity of only clinical isolates. Based on these data, we concluded that there are differences in pathogenicity potential among isolates of this subspecies, and some environmental isolates have the potential to become highly pathogenic.

1. Introduction

Photobacterium damselae subsp. *damselae* was first identified as "an unnamed marine *Vibrio*" [1] when isolated and identified as the cause of a human infectious case in 1971. Upon isolation from skin ulcers of damselfish [2], this organism was named *Vibrio damsela*. Following 5S rRNA sequence analysis, it was assigned to the new genus *Listonella* [3], and following analysis of phenotypic traits, it was reassigned to the genus *Photobacterium* as *Photobacterium damselae* [4]. At the same time, during surveys of histamine-producing bacteria [5–7], an unknown species was isolated and named *Photobacterium histaminum* as a new histamine-producing species [8]. Later, this species was considered to be a synonym of *Photobacterium damselae* subsp. *damselae* based on DNA–DNA hybridization and phenotypic study [9].

Another fish pathogen, *Pasteurella piscicida* [10], was found to be closely related to this species by 16S rRNA sequence and DNA–DNA hybridization data and was reassigned to genus *Photobacterium* [11]. Accordingly, *P. damselae* was proposed to comprise two subspecies; *P. damselae* subsp. *damselae* and *P. damselae* subsp. *piscicida*, although phenotypical data clearly distinguished these two subspecies [12].

P. damselae subsp. *damselae* has been recognized as an opportunistic pathogen for a wide variety of hosts such as a broad range of fish [13–16] and mammals [17], including humans [1]. In human cases, once infected, most patients become critical and many fatalities occur despite antibiotic treatments at the early infection stage [18–24]. Although some human infectious cases have occurred in people with notable medical histories [18,22,23], people with no underlying illnesses commonly suffer serious damages [1,23].

Previous reports on surveys of histamine-producing bacteria showed an occurrence rate of this bacterium of $1–10^3$ CFU l^{-1} in seawater around Tokyo, Japan for this species [25]. In other surveys, this species has been isolated from a wide range of environments such as estuarine and marine water, sediment, and healthy aquatic animals [26,27]. In Spain, a survey of five different fish farms

* Corresponding author. Tel./fax: +81 3 5463 0603.
E-mail address: kimubo@kaiyodai.ac.jp (B. Kimura).
[1] Present address: Yamawaki Gakuen Junior College, 4-10-36 Akasaka, Minato, Tokyo 107-8371, Japan.

0882-4010/$ – see front matter © 2008 Elsevier Ltd. All rights reserved.
doi:10.1016/j.micpath.2008.04.008

showed detection rates of 10% in asymptomatic gilthead sea bream and 6% in sea bass with rates that were even higher in warm months [13]. Furthermore, a number of marine animal diseases associated with this organism have been reported around the world [16]. However, only a few human infectious cases linked to either consumption of contaminated seafood [22] or wound infections have been reported so far. Given the wide distribution and high occurrence rate of this bacterium, the number of human infectious cases is relatively low. Moreover, different levels of symptom development have been observed among infected people; that is, some infected people die within a few days of infection despite early intervention, while some make full recoveries. This suggests that there are different levels of virulence potential for humans within this species with a high prevalence of members in the marine environment that are either not pathogenic or weakly pathogenic toward humans, while only a portion of strains possess strong pathogenicity. In fact, the virulence potential of this organism for fish has been reported to be species-specific [14,28].

In our previous study [23], we encounteredtwo fatal cases of wound infections caused by *P. damselae* subsp. *damselae*. The patients developed multiple organ failure within 20–36 h after the onset of initial symptoms. While one victim had a history of diabetes mellitus, the other had no remarkable medical history. Using these deadly clinical isolates of this species and other isolates from the environment, we investigated the genotypic and phenotypic differences between clinical and environmental isolates, as well as their pathogenicity for mice to evaluate pathogenic potential of *P.damselae* subsp. *damselae* isolates for humans.

2. Results

2.1. Phylogenetic analysis with gyrB, toxR and ompU genes

An UPGMA dendrogram was constructed for 15 isolates (13 environmental andtwo clinical) of *P. damselae* subsp. *damselae* and 4 of *P. damselae* subsp. *piscicida* based on composite data of partial sequences ofthree housekeeping genes (Fig. 1): *gyrB*, *toxR* and *ompU*. Thesethree genes were selected because they have been reported to be suitable for phylogenetic studies of *Vibrio* species, which are evolutionally close to *Photobacterium* species [29–31]. Amplification of *toxR* and *ompU* failed for other *Photobacterium* strains despite trials with different primers and amplification conditions. While *P. damselae* subsp. *piscicida* strains showed 100% identical sequences for allthree loci, those of *P. damselae* subsp. *damselae* strains were diverse, having nine distinct sequences among 15 isolates at each locus with similarity values of >97.8%, >94.1%, and >62.8% in *gyrB*, *toxR*, and *ompU*, respectively. Althoughtwo clinical *P. damselae* subsp. *damselae* strains showed distinct sequences for allthree loci, they had high similarity values in *gyrB* and *ompU* of 99.0% and 99.1%, respectively. Moreover, deduced amino acid sequences were 100% identical in thesetwo isolates for *gyrB* whereasthree and only one amino acid residues were different in *toxR* and *ompU*, respectively. This close relationship between thesetwo clinical isolates is shown in the dendrogram (Fig. 1). These clinical isolates, together with one environmental isolate, clustered together and distinctly from other environmental isolates and *P. damselae* subsp. *piscicida* isolates.

Similarity values between *P. damselae* subsp. *piscicida* and *P. damselae* subsp. *damselae* were >88.0%, indicating their close relationship.

2.2. Ribotyping

Using the automated RiboPrinter microbial characterization system as a typing system for members of this genus, all the *Photobacterium damselae* subsp. *damselae* isolates were shown to share a similar ribotype with similarity values of >95.5% and sharing one visible strong band (Fig. 2). In particular,two clinical isolates, PDA1 and PDA2, showed significant similarity (99.2%). All the *P. damselae* subsp. *piscicida* formed a single cluster, which is closer to *P. damselae* subsp. *damselae* than to other *Photobacterium* spp.

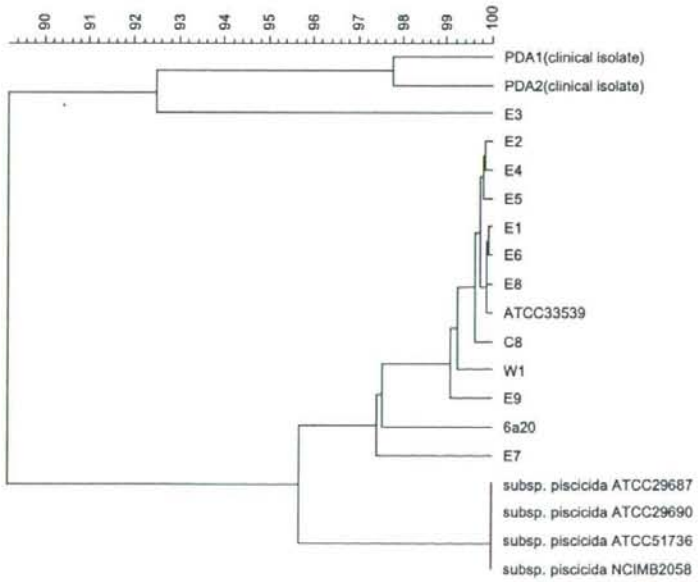

Fig. 1. UPGMA dendrogram constructed based on composite sequence data of *gyrB*, *toxR*, and *ompU* genes using Bionumerics software. Similarity percentages are shown above the dendrogram.

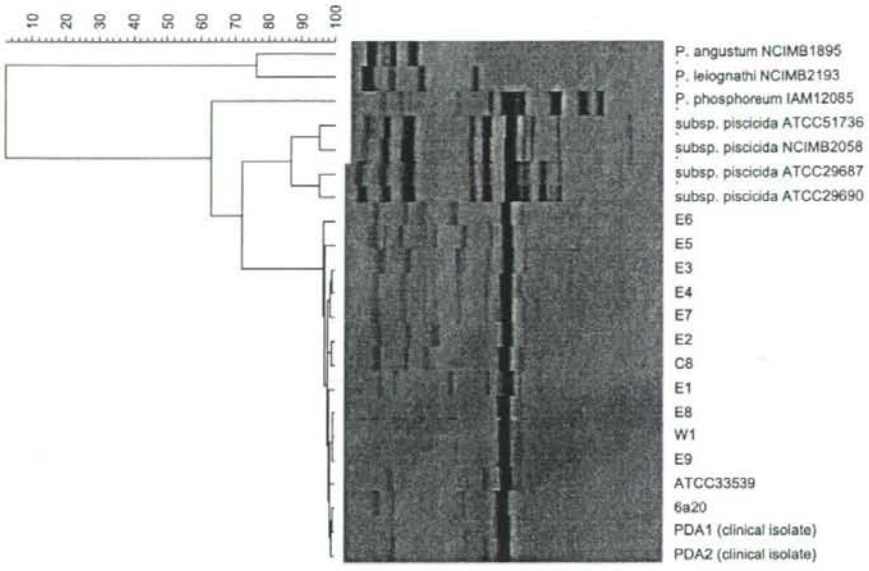

Fig. 2. UPGMA dendrogram constructed based on ribotyping. Dendrogram was constructed using Bionumerics software based on the image obtained by automated RiboPrinter system. Similarity percentages are shown above the dendrogram.

2.3. AFLP analysis

The AFLP profiles clearly separated *P. damselae* from other *Photobacterium* spp. in the dendrogram (Fig. 3). *P. damselae* subsp. *damselae* and *P. damselae* subsp. *piscicida* clustered together, with the constituents of each subspecies grouped with each other. In this dendrogram, thetwo clinical isolates of *P. damselae* subsp. *damselae*, PDA1 and PDA2, closely clustered with a similarity value of 89.4. The other three *Photobacterium* spp., *P. angustum*, *P. leiognathi*, and *P. phosphoreum*, were clearly outgrouped, indicating the close relationship of *P. damselae* subsp. *piscicida* and *P. damselae* subsp. *damselae* as subspecies.

2.4. PFGE

The PFGE banding patterns were very heterogeneous among the analyzed isolates without showing any specific pattern in common (Fig. 4). P. *damselae*, including both subspecies *damselae* and

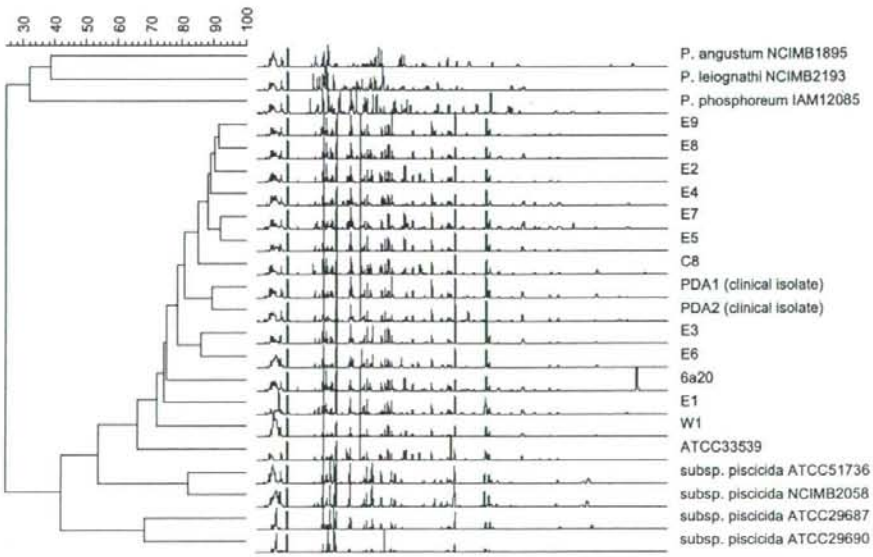

Fig. 3. UPGMA dendrogram constructed based on AFLP analysis. Dendrogram was constructed using Bionumerics software based on the densitometric values obtained by GeneScan Analysis software following electrophoresis. Similarity percentages are shown above the dendrogram.

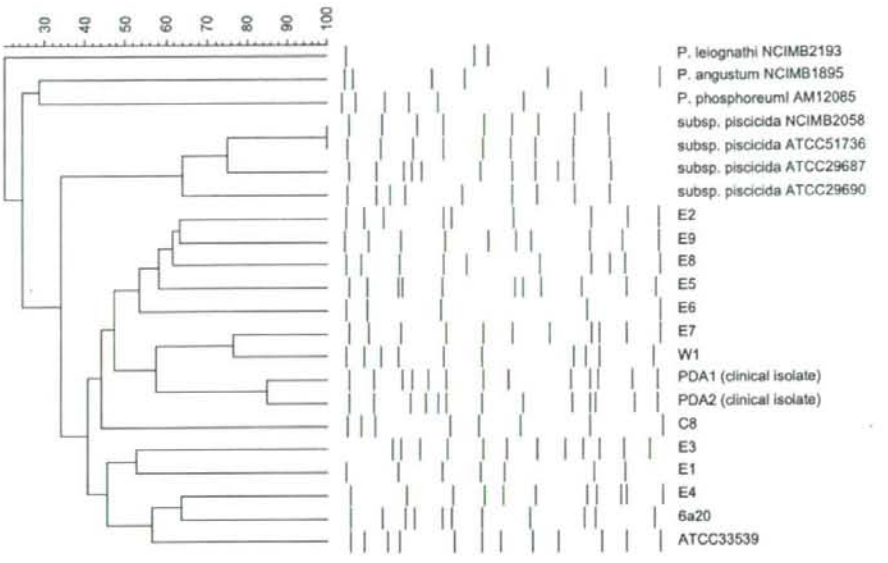

Fig. 4. UPGMA dendrogram constructed using Bionumerics software based on the electrophoretic image in the PFGE analysis. Similarity percentages are shown above the dendrogram.

piscicida, formed a single, large cluster, positioned distinctly from other *Photobacterium* spp. Within this large cluster, the two subspecies formed two different small clusters. Whereas very heterogeneous pattern was shown among *P. damselae* subsp. *damselae* isolates, thetwo clinical isolates of *P. damselae* subsp. *damselae*, PDA1 and PDA2, were positioned relatively closely to each other with a similarity value of 84.6.

2.5. Biochemical properties

A dendrogram based on biochemical property profiles (Table 3) was constructed for *Photobacterium* strains (Fig. 5). Whereas *P. damselae* subsp. *damselae* environmental strains showed highly similar profiles (similarity values of $\geq$82.8),two clinical strains of this species, PDA1 and PDA2, showed profiles distinct from these environmental strains. This distinction was reflected in the formation of a cluster comprised of thetwo clinical strains separate from that of the environmental strains in the dendrogram. The four isolates of *P. damselae* subsp. *piscicida* formed a single cluster, which is distant from the cluster of *P. damselae* subsp. *damselae* isolates (Fig. 5). This placement indicates the high degree of differences in the phenotypic characteristics between these subspecies (Table 1).

2.6. Hemolytic activities

The hemolytic activities of *P. damselae* subsp. *damselae* were roughly divided into two groups based on hemolytic halo diameter (Table 1): large halo, 7–8 mm and small halo, 2–3 mm. Thetwo clinical isolates of this species, PDA1 and PDA2, along with four environmental strains, showed large haloes, whereas the majority of environmental strains (9/13) showed small ones. The other *Photobacterium* strains, including *P. damselae* subsp. *piscicida* strains, showed no hemolytic activity to sheep erythrocytes.

2.7. Mouse virulence

The LD_{50} values of all the tested *P. damselae* subsp. *damselae* isolates ranged from 2.8×10^8 to 1.5×10^6 (Table 1). The lowest LD_{50} values, 2.4×10^6 and 1.5×10^6, were recorded for PDA1 and PDA2, respectively, indicating their strong pathogenicity for mice. These were 1–2 orders of magnitude lower than those of environmental strains where LD_{50} values ranged from 1.0×10^7 to 2.8×10^8. For other *Photobacterium* spp. isolates, including those of *P. damselae* subsp. *piscicida*, no mortality of mice was observed even for inoculation of $\geq 10^8$ CFU.

Animal mortality was monitored for 7 days, but mice either died within 24 h of inoculation or remained alive throughout the 7-day test period.

3. Discussion

We have previously encountered two cases of human infections of *Photobacterium damselae* subsp. *damselae* [23]. Both patients died, which is shocking since this bacterium is ubiquitous in aquatic environments and is often isolated from fish [32]. The known incidence of these bacteria raises the question of whether environmental isolates are as pathogenic as clinical isolates—very important information for preventing further infectious cases.

Using genomic typing methods of sequencing analysis, ribotyping, AFLP and PFGE, genomic diversity among *P. damselae* subsp. *damselae* isolates was characterized. Among the very diverse profiles,two clinical isolates, PDA1 and PDA2, had relatively similar genotypes, as shown in the dendrograms (Figs. 1–4). Although the venues of infection caused by these two isolates were distant, Okinawa prefecture and Okayama prefecture in Japan, it is possible that they were recently derived from a common progenitor. However, no visualized band or banding patterns or sequences specific to only clinical isolates were observed. The placement of clinical isolates among environmental isolates in the dendrograms demonstrates that although clinical isolates are closely related genetically, they are not clearly distinguishable from environmental isolates. Although they were clearly separated from most of the environmental strains in sequence analysis, they were still clustered together with one environmental isolate (Fig. 1).

Compared to these genotypic characteristics, the phenotypic typing showed distinct profiles for clinical isolates of *P. damselae*

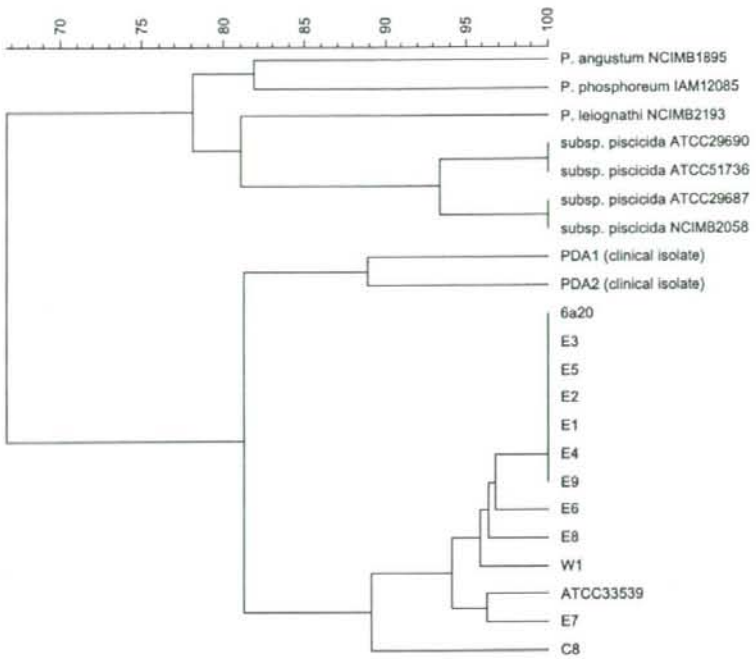

Fig. 5. UPGMA dendrogram constructed based on biochemical properties of the isolates. The obtained data using API 20E and API 50CHE were transferred into Bionumerics software to construct the dendrogram. Similarity percentages are shown above the dendrogram.

subsp. *damselae*. In a dendrogram constructed based on biochemical property profiles (Fig. 5), clinical isolates not only showed a relatively close relatedness to each other as shown in the dendrograms for the genomic typing, but they also formed a cluster clearly distinct from that of environmental isolates. This is impressive because such a clear distinction was not observed in analysis of genotypes. The clinical isolates also showed distinct characteristics in pathogenicity profiles for mice compared to environmental isolates (Table 1). One explanation of this inconsistency between the results based on genotypic and phenotypic data is that divergence of clinical strains from environmental ones is a recent event and these phenotypic differences are still so small that they are not detected by whole genome typing techniques such as PFGE and AFLP. Ribotyping showed even smaller differences between clinical and environmental isolates because rDNA is highly conserved and evolves slowly [33,34]. On the other hand, sequencing analysis of the *gyrB*, *toxR*, and *ompU* genes showed larger differences between clinical and environmental isolates. Previously, the *gyrB* gene was proposed as a suitable phylogenetic marker for the classification of bacteria because the molecular evolutionary rate of the *gyrB* gene is higher than that of 16S rDNA [34]. The same is probably true for *toxR* and *ompU* genes, as is shown in the dendrogram (Fig. 5).

Table 1
Genus *Photobacterium* strains used in this study and their pathogenic characteristics

Strain	Source	Hemolytic activity[a]	LD_{50} (CFU/mouse)
P. damselae subsp. *damselae*			
PDA1	Clinical	L	2.4×10^6
PDA2	Clinical	L	1.5×10^6
ATCC 33539	Damselfish	S	8.7×10^7
E1	Horse mackerel	S	2.8×10^8
E2	Horse mackerel	S	6.4×10^7
E3	Horse mackerel	L	2.0×10^7
E4	Horse mackerel	S	9.3×10^7
E5	Horse mackerel	S	1.9×10^8
E6	Horse mackerel	S	1.8×10^8
E7	Horse mackerel	L	1.2×10^7
6a20	Horse mackerel	S	9.9×10^7
E8	Sardine	L	1.0×10^7
E9	Sardine	S	2.7×10^8
C8	Labracoglossid fish	S	2.5×10^8
W1	Sea water	L	1.6×10^8
P. damselae subsp. *piscicida*			
ATCC 29687	Yellowtail	ND[b]	ND[c]
ATCC 29690	Yellowtail	ND	ND
ATCC 51736	Yellowtail	ND	ND
NCIMB 2058	Yellowtail	ND	ND
P. angustum NCIMB 1895	Seawater	ND	ND
P. leiognathi NCIMB 2193	Teleostean fish	ND	ND
P. phosphoreum IAM 12085	Cock rhynchus	ND	ND

[a] L, large hemolytic halo; S, small hemolytic halo.
[b] ND, hemolytic activity was not detected.
[c] ND, LD_{50} was greater than the maximum dose used.

Pathogenicity of *P. damselae* subsp. *damselae* isolates for mice and hemolytic activity were positively correlated (Table 1); except for strain W1, the remaining five strains with large hemolytic haloes ranked among the five most pathogenic strains for mice. This correlation was previously demonstrated for LD_{50} values for mice and hemolytic activities for mouse erythrocytes [35]. Although this and another report [36] showed much weaker sensitivity of sheep erythrocytes to *Photobacterium damselae* subsp. *damselae* compared to mouse and rat erythrocytes, we demonstrated a correlation between hemolytic activity for sheep erythrocytes and pathogenicity for mice. Other researchers have categorized human clinical isolates into highly virulent strain groups because of their relatively low LD_{50} values for mice and fish

[28,37] and their strong hemolytic activity [37]. Likewise, the two human clinical isolates used in our study are expected to be categorized into highly pathogenic group based on their LD_{50} values and hemolytic activity. While thetwo human clinical isolates in our study were shown to be highly pathogenic, levels of pathogenicity among environmental isolates of *P. damselae* subsp. *damselae* were variable. Strongly hemolytic isolates, such as E3, E7, E8, had stronger pathogenicity for mice compared to other environmental isolates (including strongly hemolytic strain W1). Although these isolates did not specifically group together in genomic typing (Figs. 1–4), these could be categorized as moderately pathogenic isolates. We also analyzed the plasmid contents of *P. damselae* subsp. *damselae* isolates used in this study. Plasmid contents were observed in all of the strongly hemolytic isolates, but not in weakly hemolytic ones (except ATCC 33539, which was weakly hemolytic but had a plasmid) (data not shown), indicating a contribution of plasmid contents to hemolytic activities. This needs further analysis for determination.

Our genotypic and phenotypic analyses of *P. damselae* subsp. *damselae* isolates and four *P. damselae* subsp. *piscicida* isolates show that thesetwo subspecies are closely related based on genotypes but distinct in phenotypic characteristics (Figs. 1–5), consistent with previous reports. Previously Gauthier et al. [11] proposed *P. damselae* subsp. *piscicida* as a subspecies of *P. damselae* based on its genetic relatedness to *P. damselae* subsp. *damselae*, and later Thyssen et al. [38] concurred based on AFLP and DNA–DNA hybridization analyses despite the observation of phenotypical characteristics distinct from those of *P. damselae* subsp. *damselae* [12]. In our study, *P. damselae* subsp. *piscicida* had no hemolytic activity and no pathogenicity for mice (Table 1), showing characteristics different from those of *P. damselae* subsp. *damselae*. Because of this phenotypic and genotypic inconsistency, the taxonomic position of this species within *Photobacterium* spp. is still debatable.

In this study, analysis of subspecies heterogeneity revealed that genetically similar clinical and environmental isolates had substantial phenotypic variation that alters the pathogenic potential. Overall, thetwo clinical isolates of *P. damselae* subsp. *damselae* isolated from two temporally- and spatially-separated different areas were genetically close to each other and strongly pathogenic. Some environmental strains showed moderately strong pathogenicity. This leaves two possible pathways for future infections. One is that a strongly pathogenic isolate multiplies and proliferates over a wide geographic range, as PDA1 and PDA2 might have done. Another is that moderately pathogenic strains turn into strongly pathogenic strains. In either case, sporadic or even epidemic cases can happen, and it can be a big issue since this bacterium is known to have a potential to cause fatal disease. However, our analysis of pathogenic strains was limited totwo clinical isolates, both of which were isolated in Japan. It may be necessary to analyze a larger number of geographically diverse isolates in order to produce more convincing results. Also, factors affecting the pathogenic potential of *P. damselae* subsp. *damselae* isolates, such as ability to colonize inside hosts, require further investigation.

4. Materials and methods

4.1. Bacterial strains

The 22 bacterial strains used in this study are summarized in Table 1. One strain of *Photobacterium damselae* subsp. *damselae* and the other *Photobacterium* spp. strains were obtained from the following collections: American Type Culture Collection (ATCC; Manassas, VA, USA), the Institute of Molecular and Cellular Biosciences (IAM; Tokyo, Japan), and National Collections of Industrial, Food and Marine Bacteria Japan (NCIMB; Shizuoka, Japan). *P. damselae* subsp. *damselae* clinical strains were obtained as described previously [23], and environmental isolates were collected from different types of fish and seawater in Japan between 2002 and 2003. Environmental isolates were screened for histamine forming activity as described previously [39]. Briefly, fresh skinned fish fillets were obtained from various grocery stores in and around Tokyo, Japan. Muscle tissue (5 g) was aseptically removed from each sample and placed in 45 ml histidine broth (pH 5.0) containing (per liter) 10 g Bactopepton (Difco Laboratories, Detroit, MI, USA), 3 g yeast extract (Difco), 5 g glucose and 5 g L-histidine (Wako Pure Chemical Industries, Osaka, Japan) in 50% artificial sea water (ASW) [4]. The homogenate of the mixture was incubated at 25 °C for 24 h and each culture was assayed for the presence of histamine using paper chromatography as described previously [40]. Briefly, 5 μl of the culture was applied to Advantec filter paper (No. 51B, 40 cm × 40 cm) (Toyo Roshi, Tokyo, Japan), and a solvent consisting of butanol and 10% NH_4OH (1:1) was applied following by spraying Pauly's diazo reagent. Samples identified as being positive for histamine were incubated on Niven's agar [41] supplemented with 50% ASW and the colonies light purple in color were identified using the API ID 32E (bioMérieux, Marcy l'Etoile, France) following the manufacturer's instructions.

Isolates identification was further confirmed by amplifying and sequencing approximately 400–450 bp of 16S ribosomal DNA (rDNA) (position 50–450 or –500 [*Escherichia coli* numbering]). Amplification was conducted using universal primers 27F and 1492R [42], and the amplification products were purified for use in direct sequencing with primer 27F. Resulting sequences were then used to search the DNA DataBank of Japan (DDBJ; Shizuoka, Japan) (http://www.ddbj.nig.ac.jp) by the BLAST 2.0 algorithm to confirm identification.

Isolated strains were stored in a microbank (Aska Diagnostics, Tokyo, Japan) at −80 °C. One day prior to each experiment, the frozen culture was transferred into enrichment broth for use.

4.2. DNA extraction

Bacterial strains were cultured in enriched brain heart infusion broth (BHI; Becton Dickinson, Sparks, MD) supplemented with 50% ASW (BHI-1) and DNA was extracted using the phenol–chloroform and ethanol precipitation [43]. Briefly, a 1-ml sample of enriched culture was centrifuged at 10,000 × *g* for 10 min, the bacterial cells were incubated in 567 μl of Tris–EDTA buffer containing lysozyme (2 mg ml^{-1}) for 1 h at 37 °C, and cells were lysed by adding 30 μl of 10% (w/v) sodium dodecyl sulfate and 3 μl of 20 mg proteinase K μl^{-1} followed by incubation for 1 h at 37 °C. Next, 100 μl of 5 M NaCl was added, and DNA was extracted with chloroform–isoamyl alcohol (24:1) followed by phenol–chloroform–isoamyl alcohol (25:24:1). DNA was then precipitated with isopropanol, washed with 70% ethanol, and dried. Purified DNA samples were resuspended in Tris-EDTA buffer and used as DNA templates.

4.3. Sequencing analysis of gyrB, toxR and ompU genes

All *Photobacterium damselae* isolates, including those of subsp. *damselae* and subsp. *piscicida*, were sequenced for *gyrB, toxR and ompU* genes. PCR primers used and the amplification conditions of *gyrB, toxR and ompU* genes are shown in Table 2. Primers used to amplify the *gyrB* gene were from a previous study [34], and all other primers were designed in this study (Table 2). PCR amplification was performed in 100-μl reaction mixtures: 10 mM Tris–HCl (pH 8.3), 50 mM KCl, 1.5 mM $MgCl_2$, 20 pmol of each primer, 0.2 mM each of the four dNTPs, 0.5 U Taq DNA polymerase (Takara, Shiga, Japan), and template DNA (50 ng). Amplifications were carried out with an initial denaturation at 94 °C for 5 min, a final extension at 72 °C for 4 min, and thermal cycle programs modified to each amplification target (Table 2) in a GeneAmp PCR 9700 thermal

Table 2
Amplification and sequence primers and PCR conditions

Gene	Primer		Reference	PCR conditions	
	Primer name[a]	Sequence		No. of cycles	Cycle steps
gyrB	UP-1	CAYGCXGGXGGXAARTTYGA	Yamamoto et al. (1995)	30	94 °C for 30 s, 60 °C for 1 min, 72 °C for 1.5 min
	UP-2r	CCRTCXACRTCXGCRTCXGTCAT	Yamamoto et al. (1995)		
	GYR-1f*	TAGHGCRACTCCHTACAA	This study		
	GYR-1r*	CTRGGATTYAAGAGWTCGGT	This study		
	GYR-2f*	ACCGAWCTCTTRAATCCYAG	This study		
	GYR-2r*	TTGTADGGAGTYGCDCTA	This study		
toxR	TOX-f	TTAAAGATCCAACCAAGTCTC	This study	30	94 °C for 30 s, 52 °C for 30 s, 72 °C for 30 s
	TOX-r	GTYGAAATKAGGYTCTGCCA	This study		
ompU	OMP-f	GGTATGATCACTGACTTTACCGA	This study	35	94 °C for 30 s, 55 °C for 1 min, 72 °C for 1 min
	OMP-r	TAACCTGCGTAAGTACGGAA	This study		

[a] Primers marked with * were used only for sequencing. Other primers were used for both amplification and sequencing.

cycler (Applied Biosystems, Foster City, CA, USA). PCR products (10 μl) were separated by 1% agarose gel electrophoresis at 100 V in 1× TAE buffer (pH 8.3; 40 mM Tris, 20 mM acetate, and 1 mM EDTA) along with suitable molecular markers (100-base-pair ladder, Bio-Rad, Hercules, CA, USA), and visualized with ethidium bromide under UV (245 nm) to confirm that amplification products of the expected size were produced. The amplified fragments were treated with polyethylene glycol (PEG), cooled on ice for 1 h, and pelleted by centrifugation at 15,000 × *g* for 20 min. The pellet was washed with 70% ethanol, dried, and dissolved in TE buffer. Purified DNA fragments were sequenced using an ABI 310 DNA sequencer with BigDye terminator v.3.1 cycle sequencing kits (Applied Biosystems). PCR amplification primers along with four additional primers designed for sequencing the *gyrB* gene (Table 2) were used for sequencing the partial *gyrB*, *toxR*, and *ompU* genes with varied lengths of 539 bp, 376–391 bp, and 447–474 bp, respectively. Obtained sequences were deposited in the DNA Data Bank of Japan (DDBJ; National Institute of Genetics, Shizuoka, Japan) under accession numbers AB364522 through AB364578. A preparation of composite Unweighted Pair Group Method with Arithmetic mean (UPGMA) dendrogram with average linkage (Fig. 1) and calculations of similarity values were conducted using the obtained sequences in Bionumerics v.4.0 software (Applied Maths, Sint-Martens-Latem, Belgium).

4.4. Ribotyping

All *Photobacterium* strains used in this study were characterized by automated ribotyping using a RiboPrinter microbial characterization system (Dupont Qualicon, Wilmington, DE) following the manufacturer's instructions. Briefly, isolates were streaked onto Trypticase soy agar plates (Becton Dickinson) supplemented with 50% ASW (TSA-1), then appropriate amount of colonies was used for the analysis. Following automated cell lysis, digestion of DNA with EcoRI, electrophoresis, transfer of fragments, hybridization with an *E. coli* rRNA operon probe and detection of hybridized bands with chemiluminescence, the resulting ribotypes were used to construct a dendrogram based on the Pearson product-moment correlation coefficient and UPGMA using BioNumerics software (Fig. 2).

4.5. Amplified Fragment Length Polymorphism (AFLP) analysis

All *Photobacterium* isolates used in this study were subjected to AFLP Microbial Fingerprinting Kit (Applied Biosystems). Briefly,

Table 3
Biochemical properties of *Photobacterium* spp.

Biochemical test[a]	Positive reactions (no. of isolates)					
	P. damselae subsp. *damselae*		*P. damselae* subsp. piscicida ($n = 4$)	*P. angustum* ($n = 1$)	*P. leiognathi* ($n = 1$)	*P. phosphoreum* ($n = 1$)
	Clinical strains ($n = 2$)	Environmental strains ($n = 13$)				
β-Galactosidase	–	2	–	–	–	–
Arginine dihydrolase	1	13	2	–	1	1
Lysine decarboxylase	–	–	–	–	–	1
Urease	2	13	–	–	–	–
Gelatinase	2	1	–	–	–	–
NO_3 to NO_2	2	12	–	–	1	–
Fermentation of:						
Glycerol	2	13	–	–	1	–
D-Xylose	–	–	–	–	1	–
α-Methyl-D-glucoside	2	–	–	–	–	–
Esculin	1	–	–	–	–	–
Salicin	1	–	–	–	–	–
Celliobiose	2	13	–	–	–	–
Maltose	2	13	–	1	–	1
Trehalose	2	11	–	–	–	–
Starch	–	11	–	–	–	–
Glycogen	–	1	–	–	–	–
Gentiobiose	1	–	–	–	–	–
D-Turanose	2	–	–	–	–	–
Gluconate	–	–	–	1	1	1
Sucrose	–	–	–	1	–	–

[a] Biochemical tests of ornithine decarboxylase, H_2S production, tryptophan deaminase, tryptophanase, utilization of citrate, and fermentation of D-mannitol, inositol, D-sorbitol, L-rhaminose, L-arabinose, erythritol, D-arabinose, L-arabinose, L-xylose, adonitol, β-methyl-D-xyloside, sorbose, dulcitol, α-methyl-D-mannoside, arbutin, lactose, inulin, melezitose, raffinose, xylitol, D-lyxose, D-tagatose, D-fucose, L-fucose, D-arabitol, L-arabitol, 2-keto-gluconate, 5-keto-gluconate, amygdalin, and melibiose showed negative results for all Photobacterium strains tested. Voges–Proskauer test and fermentation of ribose, galactose, fructose, mannose, *N*-acetyl glucosamine, and glucose showed positive results for all *Photobacterium* strains tested.

10 ng of extracted bacterial DNA was digested with 2.5 U of MseI and 5 U of EcoRI restriction enzymes and was subsequently ligated to MseI and EcoRI restriction site-specific adapters by overnight incubation at room temperature. Preselective PCR was carried out with a GeneAmp 9700 thermal cycler in 20-μl reaction mixtures containing 4 μl of the restriction ligation mixture, 0.5 μl of preselective MseI primer of manufacturer-defined concentration, 0.5 μl of preselective EcoRI primer of manufacturer-defined concentration, and 15 μl of AFLP Amplification Core Mix. Amplification products were diluted 20:1 with $TE_{0.1}$ buffer (20 mM Tris–HCl, 0.1 mM EDTA, pH 8.0) and used as template (1.5 μl) in selective PCR, carried out with a reaction volume of 10 μl mixture and the reaction conditions described above with MseI-selective primer and fluorescently labeled EcoRI-selective primer. MseI and EcoRI primers containing adjacent nucleotide A, C, G or T were tested for optimization. Aliquots (0.5 μl) of selective amplification products were mixed with 25 μl of deionized formamide and 1 μl of GeneScan-500 [ROX] size standard (Applied Biosystems), denatured at 95 °C for 3 min and immediately cooled on ice. AFLP capillary electrophoresis was performed on an ABI Prism 310 Genetic Analyzer (Applied Biosystems). After electrophoresis, the AFLP patterns were automatically analyzed using GeneScan Analysis software (Applied Biosystems). Densitometric values were transferred to the BioNumerics software and cluster analysis was performed using Pearson coefficients and the UPGMA clustering algorithm (Fig. 3).

4.6. Pulsed-field gel electrophoresis (PFGE)

Of eight restriction endonucleases tested under numerous electrophoretic conditions, only SfiI used under the condition described below generated fragment patterns appropriate for differentiating *Photobacterium* strains. Bacterial plugs were prepared using the Bio-Rad CHEF Bacterial Genomic DNA Plug Kit (Bio-Rad) following the manufacturer's instructions with a minor modification. Briefly, isolated strains were cultured in BHI-1 at 30 °C until reaching OD_{600} of 0.8. Subsamples (1 ml) were incubated with chloramphenicol at a final concentration of 180 μg ml^{-1} for another 1 h. The suspensions were centrifuged at 10,000 × *g* for 3 min at 4 °C. Pellets were resuspended in Suspension Buffer to which 2% CleanCut agarose was added to achieve a final concentration of 1%. The cell–agarose mixture was transferred to disposable plug molds and maintained at 4 °C for 10 min for the mixture to solidify. The plugs were pushed out into wells containing 12 μl of lysozyme stock and 300 μl of lysozyme buffer in 24-well polystyrene plates. After incubating at 37 °C for 2 h with gentle agitation, the lysozyme solution was removed. The plugs were washed with sterile water, and incubated overnight at 50 °C with 300 μl of Proteinase K reaction buffer and 12 μl of Proteinase K stock. The plugs were washed four times in 1× Wash Buffer, with each wash lasting 1 h and 1 mM phenylmethanesulfonylfluoride replacing 1× Wash Buffer in the third wash. The buffer was aspirated and 30 U of SfiI with the appropriate amount of buffer was added to each plug. The plugs were incubated in the presence of this enzyme for 17 h, cut into appropriate sizes, loaded into the wells of the agarose gel (1% Seakem Gold Agarose, Cambrex, Rockland, ME, USA), and electrophoresed for 18 h in 0.5 × TBE buffer at 14 °C with an applied voltage of 6 V with Bio-Rad CHEF-DR II system. Initial time of 5 s and final time of 50 s were selected. DNA bands were visualized under UV light after ethidium bromide staining. A dendrogram was constructed using BioNumerics software based on Dice coefficient and UPGMA parameters (Fig. 4).

4.7. Biochemical properties

Biochemical properties of the *Photobacterium* isolates were characterized using API commercial test kit (Table 1): API 20E and API 50CHE (bioMérieux). The tests were performed following the manufacturer's instructions with modifications in the suspension broth, length and temperature of incubation. Briefly, colonies grown on BHI-1 agar plates for each isolate were suspended in media specific to each test, to which NaCl was supplemented to a final concentration of 1.5% (w/v). Bacterial suspensions were inoculated into strips for each test following manufacturer's instructions and incubated at 26 °C for 72 h according to Thyssen et al. (1998). Every questionable test result was repeated twice or more. A dendrogram was constructed using BioNumerics software based on Dice coefficient and UPGMA (Fig. 5).

4.8. Hemolytic activity assay

Hemolytic activity was assayed on sheep blood agar for all *Photobacterium* isolates used in this study. Sheep blood was selected because it has been shown to have the same level of susceptibility to *P. damselae* subsp. *damselae* as human blood does [35,36]. Each strain was grown in TSB-1 to early log phase. The culture was streaked onto TSA-1 plates, allowed to dry for 10 min, then overlaid with 6 ml of soft TSA-1 supplemented with 5% sheep blood, which had been melted and kept warm. After solidification, the plates were incubated at 30 °C for 24 h, and then the diameter of hemolytic halo was measured in millimeters (Table 1). Experiments were done in triplicate.

4.9. Mouse virulence

Male ddY 4-week-old mice (Sankyo Labo Service, Tokyo, Japan) each weighing 20–22 g were used to assay pathogenicity. Mice were allowed free access to water and chow diet throughout the experimental period. Each bacterial strain was cultured to mid-log growth phase in BHI-1 broth, and diluted 10-fold to produce cell suspensions in the range of 10^5–10^8 CFU 0.1 ml^{-1} in phosphate-buffered saline. Mice were divided into groups of five each and injected intraperitoneally with 0.1 ml of either sterile PBS (control) or cell suspensions at each concentration. Bacterial counts of the inocula were confirmed by plating serially diluted cultures onto BHI-1 agar in duplicate using a spiral plater (IUL S.A., Barcelona, Spain). Mortality was observed for 7 days and LD_{50} was calculated for each strain using the method of Reed and Muench [44].

Acknowledgements

We thank Chika Saito and Chikako Kamimura for technical support.This work was partly supported by Japanese Ministry of Health, Labour and Welfare (H20-011).

References

[1] Morris Jr JG, Wilson R, Hollis DG, Weaver RE, Miller HG, Tacket CO, et al. Illness caused by *Vibrio damselae* and Vibrio hollisae. Lancet 1982;i:1291–7.
[2] Love M, Teebken-Fisher D, Hose JE, Farmer III JJ, Hickman FW, Fanning FW. *Vibrio damselae*, marine bacterium causes skin ulcers on the damselfish *Chromis punctipinnis*. Science 1981;214:1139–40.
[3] MacDonell MT, Colwell RR. Phylogeny of the *Vibrionaceae*, and recommendation for two new genera, *Listonella* and *Shewanella*. Syst Appl Microbiol 1985; 6:171–82.
[4] Smith SK, Sutton DC, Fuerst JA, Reichelt JL. Evaluation of the genus *Listonella* and reassignment of *Listonella damselae* (Love et al.) MacDonell and Colwell to the genus *Photobacterium* as *Photobacterium damselae* comb. nov. with an emended description. Int J Syst Bacteriol 1991;41:529–34.
[5] Okuzumi M, Okuda S, Awano S. Isolation of psychrophilic and halophilic histamine-forming bacteria from *Scomber japonicus*. Bull Jpn Soc Sci Fish 1981;47: 1591–8.
[6] Yoguchi R, Okuzumi M, Fujii T. Seasonal variation in numbers of mesophilic and halophilic histamine-forming bacteria in inshore of Tokyo Bay and Sagami Bay. Nippon Suisan Gakkaishi 1990;56:1467–72. In Japanese.
[7] Yoguchi R, Okuzumi M, Fujii T. Seasonal variation in numbers of mesophilic and halophilic histamine-forming bacteria on marine fish. Nippon Suisan Gakkaishi 1990;56:1473–9. In Japanese.

[8] Okuzumi M, Hiraishi A, Kobayashi T, Fujii T. *Photobacterium histaminum* sp. nov., a histamine-producing marine bacterium. Int J Syst Bacteriol 1994;44:631–6.
[9] Kimura B, Hokimoto S, Takahashi H, Fujii T. *Photobacterium histaminum* Okuzumi et al. 1994 is a later subjective synonym of *Photobacterium damselae* subsp. *damselae* (Love et al. 1981) Smith et al. 1991. Int J Syst Evol Microbiol 2000;50:1339–42.
[10] Janssen WA, Surgalla MJ. Morphology, physiology, and serology of a *Pasteurella* species pathogenic for white perch (*Roccus americanus*). J Bacteriol 1968;96: 1606–10.
[11] Gauthier G, Lafay B, Ruimy R, Breittmayer V, Nicolas JL, Gauthier M, et al. Small-subunit rRNA sequences and whole DNA relatedness concur for the reassignment of *Pasteurella piscicida* (Sniezko et al.) Janssen and Surgalla to the genus *Photobacterium* as *Photobacterium damselae* subsp. *piscicida* comb. nov. Int J Syst Bacteriol 1995;45:139–44.
[12] Thyssen A, Grisez L, van Houdt R, Ollevier F. Phenotypic characterization of the marine pathogen *Photobacterium damselae* subsp. *piscicida*. Int J Syst Bacteriol 1998;48:1145–51.
[13] Botella S, Pujalte MJM, Macián C, Ferrús MA, Hernández J, Garay E. Amplified fragment length polymorphism (AFLP) and biochemical typing of *Photobacteium damselae* subsp. *damselae*. J Appl Micobiol 2002;93:681–8.
[14] Fouz B, Larsen JL, Nielsen B, Barja JL, Toranzo AE. Characterization of *Vibrio damsela* strains isolated from turbot *Scophthalmus maximus* in Spain. Dis Aquat Org 1992;12:155–66.
[15] Grimes DJ, Stemmler J, Hada H, May EB, Maneval D, Hetrick FM, et al. *Vibrio* species associated with mortality of sharks held in captivity. Microb Ecol 1984; 10:2271–82.
[16] Pedersen K, Dalsgaard I, Larsen L. *Vibrio damsela* associated with diseased fish in Denmark. Appl Environ Microbiol 1997;63:3711–5.
[17] Fujioka RS, Greco SB, Cates MB, Schroeder JP. *Vibrio damselae* from wounds in bottlenose dolphins, *Tursiops truncatus*. Dis Aquat Org 1988;4:1–8.
[18] Clarridge JE, Zighelboim-Daum S. Isolation and characterization of two hemolytic phenotypes of *Vibrio damsela* associated with a fatal wound infection. J Clin Microbiol 1985;21:302–6.
[19] Fraser SL, Purcell BK, Delgado Jr B, Baker AE, Whelen AC. Rapidly fatal infection due to *Photobacterium (Vibrio) damsela*. Clin Infect Dis 1997;25:935–6.
[20] Lang M. Fatal *Vibrio damsela* bacteremia. Clin Microbiol Newslett 1992;14: 166–7.
[21] Perez-Tirse J, Levine JF, Mecca M. *Vibrio damsela*: a cause of fulminant septicemia. Arch Intern Med 1993;153:1838–40.
[22] Shin JH, Shin HG, Suh SP, Ryang DW, Rew JS, Nolte FS. Primary *Vibrio damsela* septicemia. Clin Infect Dis 1996;22:856–7.
[23] Yamane K, Asato J, Kawade N, Takahashi H, Kimura B, Arakawa Y. Two cases of fatal necrotizing fasciitis caused by *Photobacterium damsela* in Japan. J Clin Microbiol 2004;42:1370–2.
[24] Yuen KY, Ma L, Wong SSY, Ng WF. Fatal necrotizing fasciitis due to *Vibrio damsela*. Scand J Infect Dis 1993;25:659–61.
[25] Okuzumi M. Psychrophilic histamine-forming bacteria on/in marine fish. J Jpn Soc Cold Pres Food 1993;19:30–40.
[26] Buck JD. Potentially pathogenic marine *Vibrio* species in seawater and marine animals in the Sarasota, Florida, area. J Coastal Res 1990;6:943–8.
[27] Ghinsberg RC, Drasinover V, Sheinberg Y, Nitzan Y. Seasonal distribution of *Aeromonas hydrophila* and *Vibrio* species in Mediterranean coastal water and beaches: a possible health hazard. Biomed Lett 1995;51:151–9.
[28] Fouz B, Barja JL, Amaro C, Rivas C, Toranzo AE. Toxicity of the extracellular products of *Vibrio damsela* isolated from diseased fish. Curr Microbiol 1993;27: 341–7.
[29] Roux FL, Goubet A, Thompson FL, Faury N, Gay M, Swings J, et al. *Vibrio gigantis* sp. nov., isolated from the haemolymph of cultured oysters (*Crassostrea gigas*). Int J Syst Evol Microbiol 2005;55:2251–5.
[30] Franco PF, Hedreyda CT. Amplification and sequence analysis of the full length toxR gene in *Vibrio harveyi*. J Gen Appl Microbiol 2006;5:281–7.
[31] Bisharat N, Amaro C, Fouz B, Llorens A, Cohen DI. Serological and molecular characteristics of *Vibrio vulnificus* biotype 3: evidence for high clonality. Microbiology 2007;153:847–56.
[32] Takahashi H, Sato M, Kimura B, Ishikawa T, Fujii T. Evaluation of PCR-single strand conformational polymorphism analysis for identification of gram-negative histamine-producing bacteria isolated from fish. J Food Prot 2007;70: 1200–5.
[33] Osorio CR, Collins MD, Romalde JL, Toranzo AE. Characterization of the 23S and 5S rRNA genes and 23S-5S intergenic spacer region (ITS-2) of *Photobacterium damselae*. Dis Aquat Org 2004;61:33–9.
[34] Yamamoto S, Harayama S. PCR amplification and direct sequencing of *gyrB* genes with universal primers and their application to the detection and taxonomic analysis of *Pseudomonas putida* strains. Appl Environ Microbiol 1995; 61:1104–9.
[35] Kreger AS. Cytolytic activity and virulence of *Vibrio damsela*. Infect Immun 1984;44:326–31.
[36] Kothary MH, Kreger AS. Purification and characterization of an extracellular cytolysin produced by *Vibrio damsela*. Infect Immun 1985;49:25–31.
[37] Osorio CR, Romalde JL, Barja JL, Toranzo AE. Presence of phospholipase-D (*dly*) gene coding for damselysin production is not a pre-requisite for pathogenicity in *Photobacterium damselae* subsp. *damselae*. Microb Pathog 2000;28:119–26.
[38] Thyssen A, van Eygen S, Hauben L, Goris J, Swings J, Ollevier F. Application of AFLP for taxonomic and epidemiological studies of *Photobacterium damselae* subsp. *piscicida*. Int J Syst Evol Microbiol 2000;50:1013–9.
[39] Takahashi H, Kimura B, Yoshikawa M, Fujii T. Cloning and sequencing of the histidine decarboxylase genes of gram-negative, histamine-producing bacteria and their application in detection and identification of these organisms in fish. Appl Environ Microbiol 2003;69:2568–79.
[40] Miyaki T. Scombroid fish poisoning. Food Sanit Res 1954;12:7–14.
[41] Niven CF, Jeffrey MB, Corlett DA. Differential plating medium for quantitative detection of histamine-producing bacteria. Appl Environ Microbiol 1981;41: 321–2.
[42] Lane DJ. 16S/23S rRNA sequencing. In: Stackebrandt E, Goodfellow M, editors. Nucleic acid techniques in bacterial systematics. Chichester, UK: Wiley & Sons; 1991. p. 115–75.
[43] Sambrook J, Fritsch EF, Maniatis T. Molecular cloning: a laboratory manual. 2nd ed. Cold Spring Harbor, NY: Cold Spring Harbor Laboratory Press; 1989.
[44] Reed LJ, Muench H. A simple method of estimating fifty percent endpoints. Am J Hyg 1938;27:493–7.

International Journal of Food Microbiology 124 (2008) 239–249

Contents lists available at ScienceDirect

International Journal of Food Microbiology

journal homepage: www.elsevier.com/locate/ijfoodmicro

Development of a multilocus variable-number of tandem repeat typing method for *Listeria monocytogenes* serotype 4b strains

Satoko Miya [a], Bon Kimura [a,*], Miki Sato [a], Hajime Takahashi [a], Tatsuya Ishikawa [a], Takayuki Suda [a], Chikako Takakura [a], Tateo Fujii [a], Martin Wiedmann [b]

[a] Department of Food Science and Technology, Faculty of Marine Science, Tokyo University of Marine Science and Technology, 4-5-7 Konan, Minato-ku, Tokyo 108-8477, Japan
[b] Department of Food Science, Cornell University, Ithaca, New York, United States

ARTICLE INFO

Article history:
Received 11 July 2007
Received in revised form 17 March 2008
Accepted 24 March 2008

Keywords:
Listeria monocytogenes
4b
Subtyping
Epidemic clones

ABSTRACT

Listeria monocytogenes serotype 4b strains have been identified as the causative agent in many human listeriosis epidemics as well as in a considerable number of sporadic cases. Due to the genetic homogeneity of serotype 4b isolates, development of rapid subtyping methods with high discriminatory power for serotype 4b isolates is required to allow for improved outbreak detection and source tracking. In this study, multilocus variable-number tandem repeat analysis (MLVA) was developed and used to characterize 60 serotype 4b isolates from various sources. All isolates were also characterized by automated EcoRI ribotyping, single enzyme pulsed-field gel electrophoresis (PFGE) with ApaI, and a multilocus sequence typing (MLST) scheme targeting six virulence and virulence-associated genes. Discriminatory power of MLVA (as determined by Simpson Index of Discrimination) was higher than the discriminatory power of any of the other three methods. MLVA markers targeted were found to be stable and did not change when three isolates were passaged daily for 70 days. Cluster analyses of MLVA, PFGE and MLST consistently grouped the same isolates into three major clusters, each of which includes one of the three major *L. monocytogenes* epidemic clones (i.e., ECI, ECIa and ECII). We conclude that the MLVA method described here (i) provides for more discriminatory subtyping of *L. monocytogenes* serotype 4b strains than the other three methods, (ii) identifies three major groups within the serotype 4b, which are consistent with the groups identified by other subtyping methods, and (iii) is easy to interpret. Use of MLVA may thus be recommended for subtyping of serotype 4b isolates, including as a secondary more discriminatory subtyping method that could be used after initial isolate characterization by PFGE or ribotyping.

1. Introduction

Listeria monocytogenes is an ubiquitous bacterium that can cause severe invasive foodborne disease in humans. While 13 different serotypes have been identified in this organism to date, serotype 4b isolates have been responsible for most human listeriosis epidemics and are responsibly for the majority of human sporadic cases in many parts of the world (Farber and Peterkin, 1991; Schuchat et al., 1991). Serotype 4b isolates have been reported to be highly clonal and are genetically more homogeneous than other common *L. monocytogenes* serotypes (Graves et al., 1994; Mereghetti et al., 2002; O'Donoghue et al., 1995; Ridley, 1995). Specific highly clonal serotype 4b strains that have been responsible for multiple human listeriosis outbreaks have been classified into specific epidemic clones (EC), including ECI, ECIa (Kathariou, 2003), and ECII (Evans et al., 2004). The vast majority of *L. monocytogenes* serotype 4b isolates group into lineage I, which is predominant among human clinical listeriosis cases. In addition, a few atypical and genetically distinct serotype 4b isolates group into *L. monocytogenes* lineage III; while only lineage I serotype 4b strain are the focus of the study reported here, two lineage III serotype 4b isolates were also initially characterized by the MLVA method reported here.

Considering the highly clonal nature and genetic homogeneity of lineage I serotype 4b strains as well as their common involvements in human listeriosis cases and outbreaks, it is critical to develop rapid molecular subtyping methods that provide increased discrimination of these strains over existing subtyping methods. A number of molecular subtyping methods have been developed for and are commonly used for *L. monocytogenes*, including automated ribotyping, pulsed-field gel electrophoresis (PFGE), and more recently different multilocus sequence typing procedures targeting housekeeping as well as virulence genes (e.g., Cai et al., 2002; Revazishvili et al., 2004; Salcedo et al., 2003; Zhang et al., 2004; reviewed by Wiedmann, 2002). Automated ribotyping represents a highly reproducible and standardized subtyping method, which appears to be able to classify serotype 4b strains into epidemic clones as ECI and ECIa strains appear to be represented by ribotypes DUP-1038 and DUP-1042, respectively

* Corresponding author. Tel./fax: +81 3 5463 0603.
E-mail address: kimubo@kaiyodai.ac.jp (B. Kimura).

0168-1605/$ – see front matter © 2008 Elsevier B.V. All rights reserved.
doi:10.1016/j.ijfoodmicro.2008.03.023

Table 1
Subtypes and characteristics of *L. monocytogenes* isolates used in this study

Isolate no.[a]	Origin	Isolation date (day/mo/yr)[c]	MLVA cluster	MLVA type (no. of repeats) for			Ribotype	MLST type[d]	PFGE type
				TR1	TR2	TR3			
Outbreak related isolates (4b)									
CIP103322†	Human (Switzerland, 1983–87)	1987	1	22	17	9	1038B	1	6
FSL J1-003†	Human (Nova Scotia, 1981)	1981	1	19	17	9	1038B	1**	2
FSL J1-220†	Human (Boston; 1979)	1979	3	23	12	7	1042B	9**	24
FSL N1-225	Human (US; 1998–99)	1998	2B	23	22	5	1044A	17*	16
CIP103575†	Food (milk, Massachusetts, 1983)	1983	3	24	12	7	1042B	12	22
FSL J1-116†	Human (United Kingdom, 1983–87)	1988	3	23	12	7	1042B	9**	22
FSL N3-013	Food (pate; United Kingdom, 1983–87)	1988	3	12	12	7	1042B	9**	22
FSL J1-119	Human (Los Angeles, 1985)	1985	1	12	17	9	1038B	1**	6
FSL J1-110†	Food (Los Angeles, 1985)	1985	1	12	17	9	1038B	1**	6
Other isolates (4b)									
ATCC19115†	Human	N/A	3	25	12	7	1042B	9	25
CIP101821†	Human	1985	3	14	12	6	1042B	11	27
CIP102551†	Human	1986	1	23	16	9	1038B	7	6
NCTC4885†	Human	1936	1	18	17	9	1038B	6	7
NCTC9863†	Human	1956	3	23	12	7	1042B	9	23
NCTC10527†	Human	1967	3	25	12	7	1042B	9	26
FSL C1-132	Human sporadic	14-Sep-98	1	18	17	9	1038A	1	1
FSL C1-134	Human sporadic	15-Oct-98	1	21	17	9	1038B	1	3
FSL F2-021	Human sporadic	27-Jul-99	1	14	19	9	1038B	1	6
FSL F2-022	Human sporadic	3-Aug-99	2A	15	17	5	1042B	19	10
FSL F2-024	Human sporadic	4-Aug-99	2B	23	18	5	1044A	17	17
FSL F2-037	Human sporadic	23-Sep-99	1	14	19	9	1038B	1	6
FSL F2-091	Human sporadic	3-Aug-99	3	14	12	6	1042B	9	27
FSL F2-140	Human sporadic	14-Sep-99	2A	15	14	5	116-363-S-2	21	13
FSL F2-243	Human sporadic	6-Jan-00	1	14	19	9	1038B	1	6
FSL F2-372	Human sporadic	26-May-00	1	14	19	9	1038B	1	6
FSL F2-382	Human sporadic	22-Mar-00	1	13	17	9	1038B	1	5
FSL F2-420	Human sporadic	16-Jun-00	2B	14	10	5	1044A	17	16
FSL F2-427	Human sporadic	20-Jul-00	2B	23	18	5	1044A	18	17
FSL F2-475	Human sporadic	5-Aug-00	2A	16	17	5	1042B	20	12
FSL F2-480	Human sporadic	23-Aug-00	1	11	17	9	1038B	8	6
FSL F2-601	Human	2001	2A	10	17	5	1042B	25	10
FSL F2-637	Human sporadic	14-May-01	2B	23	18	5	1044A	17	14
FSL F2-642	Human sporadic	29-May-01	2A	16	17	5	1042B	20	12
FSL F2-656	Human sporadic	4-Jul-01	3	26	12	7	1042A	9	25
FSL F2-658	Human	2001	1	26	17	9	1038B	1	4
FSL F2-661	Human sporadic	20-Apr-01	3	27	12	7	1042B	9	27
FSL F2-672	Human sporadic	31-Aug-01	2B	19	21	5	1044A	17	16
FSL F2-689	Human sporadic	2001	1	9	17	9	1027C	1	6
FSL M2-042	Human sporadic	16-Feb-99	3	16	12	7	1042B	10	23
FSL J1-012†	Human	N/A	1	16	17	9	1038B	1	7
NCTC11994†	Food (soft cheese, assoc. with human case)	1986	1	18	17	9	1038B	3	8
ATCC51777†	Food (cheese)	N/A	1	18	17	9	1038B	2	8
20-5-1†	Food (cod roe)	28-Oct-04	2A	15	15	5	1042A	23	20
34-18-2†	Food (cod roe)	28-Apr-05	2A	16	15	5	1042A	16	21
Lma5†	Food (pork); plant A	N/A	2B	14	21	5	1044A	17	15
Lma7†	Food (pork); plant A	N/A	2B	14	21	5	1044A	17	14
Lmb15†	Food (pork); plant B	28-May-90	2A	11	15	5	1042A	15	19
Lmb17†	Food (pork); plant B	28-May-90	2A	11	15	5	1042A	14	18
Lmb20†	Food (pork); plant B	3-Jun-90	2B	22	21	5	1044A	17	14
Lmc1†	Food (pork), plant F	N/A	3	25	12	7	172-75-S-1	13	27
Lmc26†	Food (pork), plant C	N/A	3	15	12	7	1042B	9	27
Lmc32†	Food (pork), plant G	N/A	3	14	12	7	1042A	9	27
Lmc39†	Food (pork), plant F	N/A	3	25	12	7	172-75-S-1	9	27
FSL F2-001	Food (fresh white cheese)	28-Jun-99	2B	14	10	5	1044A	17	16
FSL F2-281	Food (white fish salad)	3-Feb-00	1	26	17	9	1027B	5	9
FSL E1-055	Animal (bovine)	1999	1	19	17	9	1038B	1	6
FSL E1-124	Animal (bovine)	1-Jun-01	1	19	17	9	1038B	4	6
FSL E1-125	Animal (caprine)	12-Jun-01	2A	15	14	5	1042B	22	12
FSL J2-039	Animal (wild turkey)	1993	2A	10	8	5	1042B	24*	11
FSL N4-289	Animal	2001	1	15	19	9	1038B	1	6
FSL F2-525[b]	Human sporadic (lineage III)	30-Aug-00	N/A	N/A[e]	14	N/A	1061A	26	28
FSL J1-158[b]	Animal (caprine) (lineage III)	Jul-97	N/A	N/A	14	N/A	10142	27	29
Other isolates (1/2a, 1/2b)									
FSL C1-117 (1/2a)	Human sporadic	9-Oct-98	N/A	16	16	9	1039C	28	30
FSL F2-029 (1/2a)	Human sporadic	29-Aug-99	N/A	8	13	9	1062D	34	31
FSL F2-048 (1/2a)	Human sporadic	24-Sep-99	N/A	21	18	9	1053A	32	32
39-17-1 (1/2a)	Food (salmon roe)	21-Jul-05	N/A	16	11	9	1030A	33	33
FSL E1-042 (1/2a)	Animal (bovine)	Apr-00	N/A	16	11	9	1030A	33	33
FSL E1-123 (1/2a)	Animal (bovine)	22-Jun-01	N/A	20	15	9	1039C	35	34